Dependence of the radio emission of air showers on the cosmic ray primary particle composition

Washington Rodrigues de Carvalho Jr.

Faculty of Physics, University of Warsaw, Poland

carvajr@gmail.com

FUW seminar
October 25th, 2024

Overview

1. Introduction to Cosmic Rays
   - Cosmic Rays (CR)
   - Extensive air showers
   - Radio emission of air showers
     - Emission Mechanisms
     - Cherenkov-like effects
     - Shower geometry, X_{max} and the radio footprint
2. Revisiting the radio LDF dependence on CR primary composition
   - Motivation or "how supervised ML is not a black-box"
   - A historically overlooked dependence
   - Simulations: How does the RLDF actually look like
   - Why does the amplitude depend on X_{max} ?
   - $\vec{E}$ scalings and loss of coherence at low air density
   - Conclusions

UNIVERSITY OF WARSAW

Section 1

Introduction to Cosmic Rays

Cosmic-ray flux and arrival direction

- Charged particles: H to ∼Fe nuclei
- Information about astrophysical objects (ch. particle astronomy)
- Deflected by galactic/extragalactic magnetic fields:
  - CRs don't point at their sources.
  - Deflection depends on Energy (E), composition (Z), distance (r) and magnetic fields (l_c, B).

$$\theta \simeq 0.8^\circ Z \left(\frac{E}{10^{20} eV}\right)^{-1} \left(\frac{r}{10 Mpc}\right)^{\frac{1}{2}} \left(\frac{l_c}{1 Mpc}\right)^{\frac{1}{2}} \left(\frac{B}{10^{-9} G}\right)$$

- Huge energy and flux ranges
- Acceleration mechanisms at UHE not fully understood

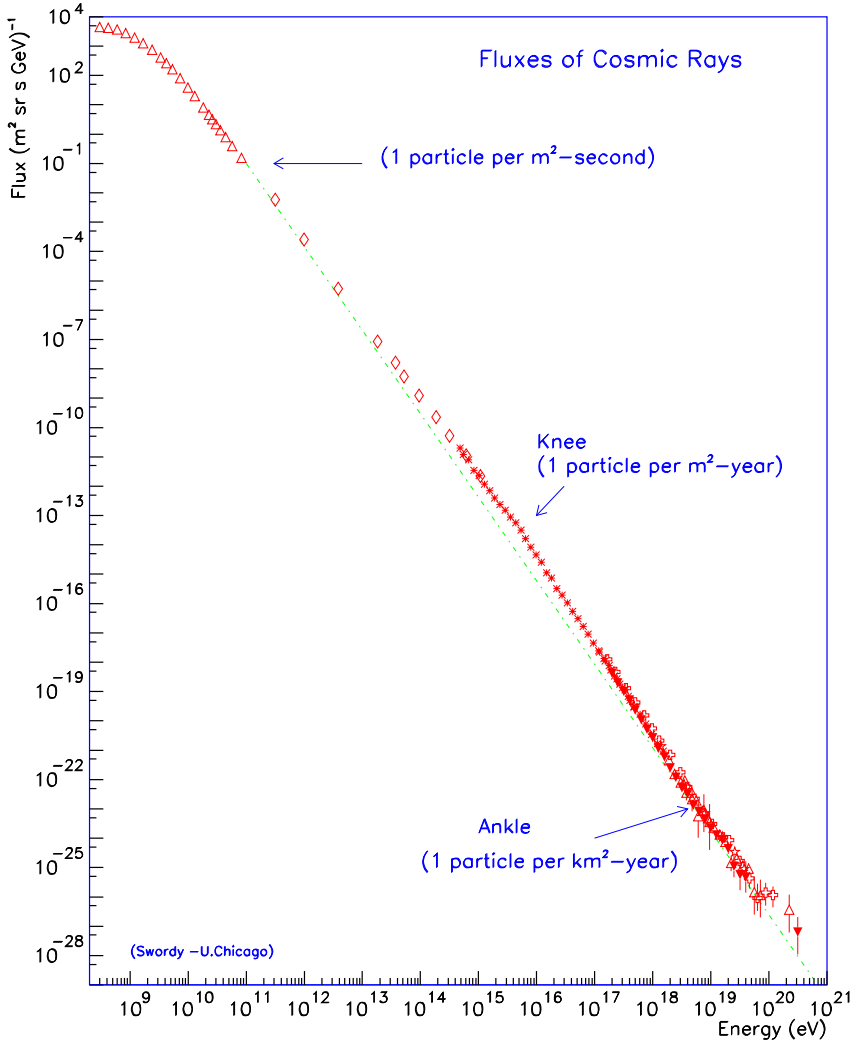

Constrain on sources: the Hillas plot

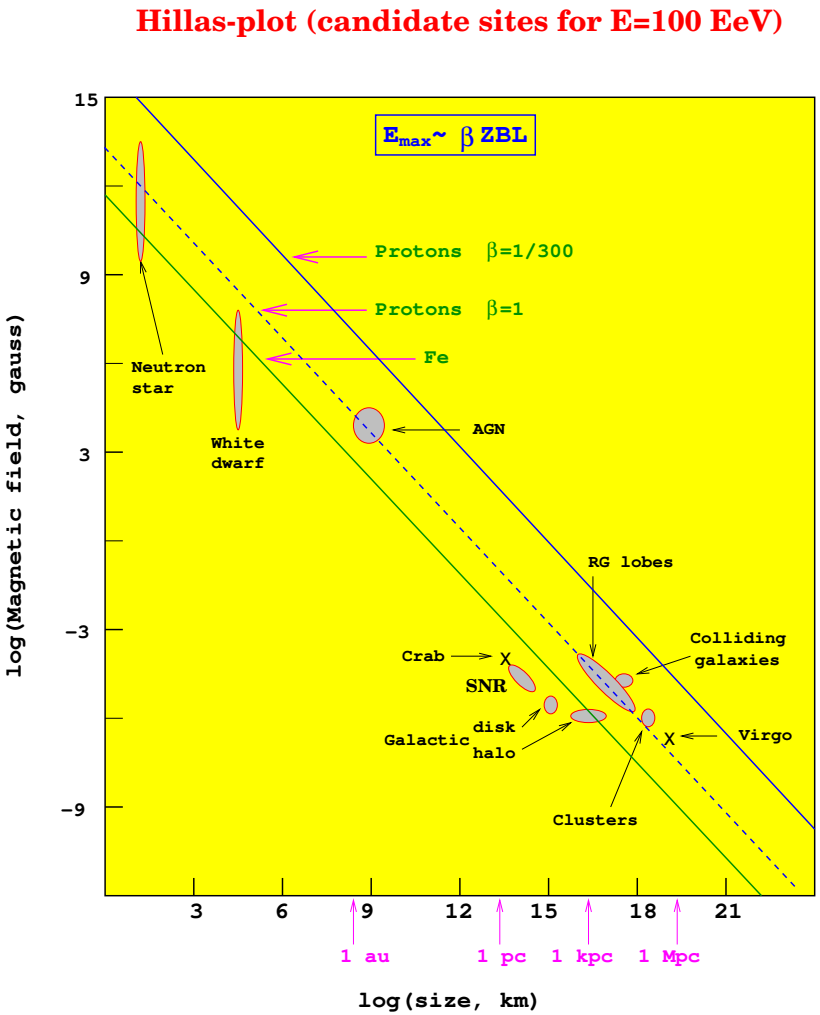

- Necessary condition: Source must be able to contain the accelerating particle
  - Larmor radius ($E_{15}/ZB_{\mu G}$) must be smaller than the source
  - Leads to a maximum energy depending on the source size L, magnetic field B and Z of primary particle
  - Given a source, heavier nuclei can be accelerated to a higher energy

$$E_{max} \cong \beta Z \left(\frac{B}{1\mu G}\right)\left(\frac{R}{1kpc}\right)\ 10^{18}\ \ eV$$

UNIVERSITY OF WARSAW

Cosmic rays have information on astrophysical objects

Cosmic rays have information on astrophysical objects

Characterization of UHE Cosmic Rays

- Arrival direction
- Energy
- Composition (p, Fe, etc...)

Cosmic rays have information on astrophysical objects

Characterization of UHE Cosmic Rays

- Arrival direction
- Energy
- Composition (p, Fe, etc...)

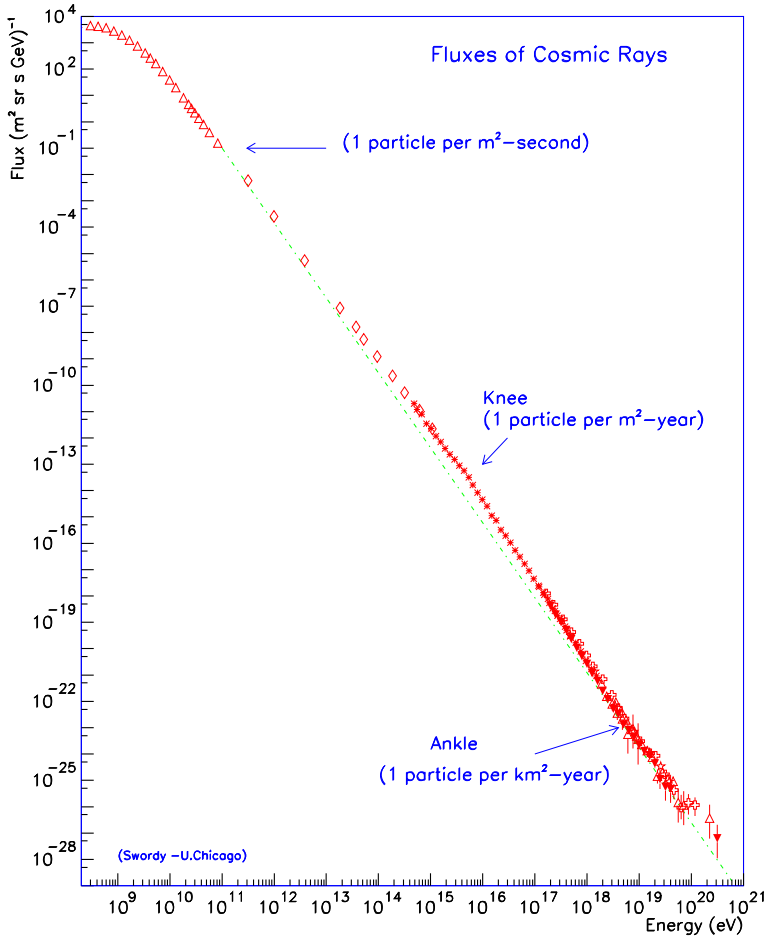

But the flux is very small!!!

Cosmic rays have information on astrophysical objects

Characterization of UHE Cosmic Rays

- Arrival direction
- Energy
- Composition (p, Fe, etc...)

Detection technique should:

- Provide large statistics:
  - Cover a large area
  - Have a large duty cycle
- Be sensitive to composition

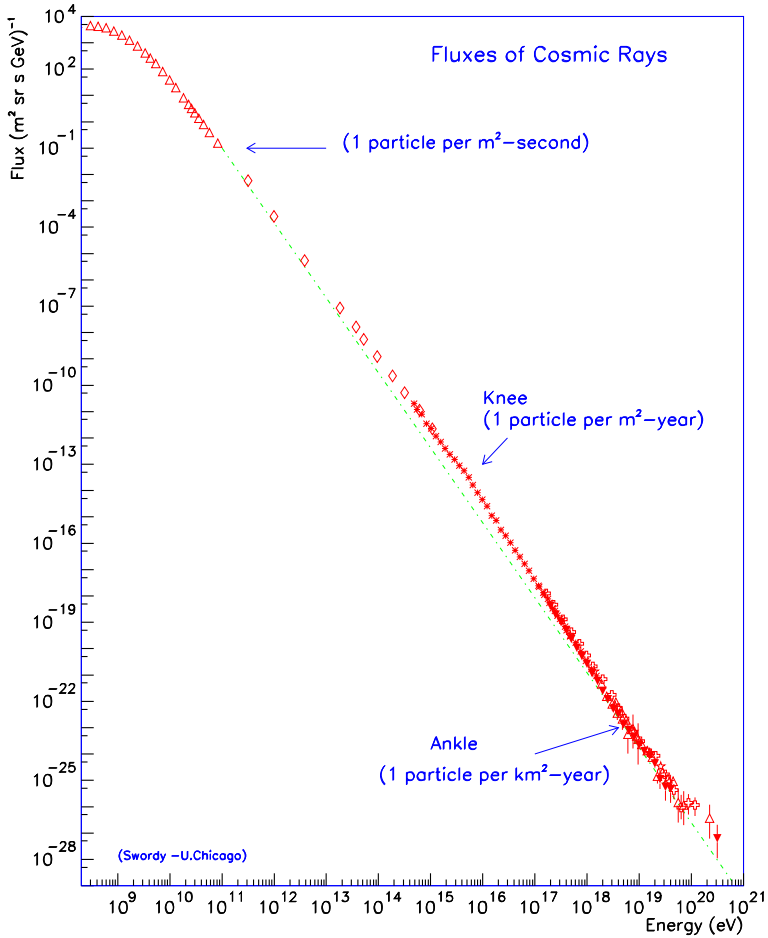

But the flux is very small!!!

Extensive Air Showers: shower scheme

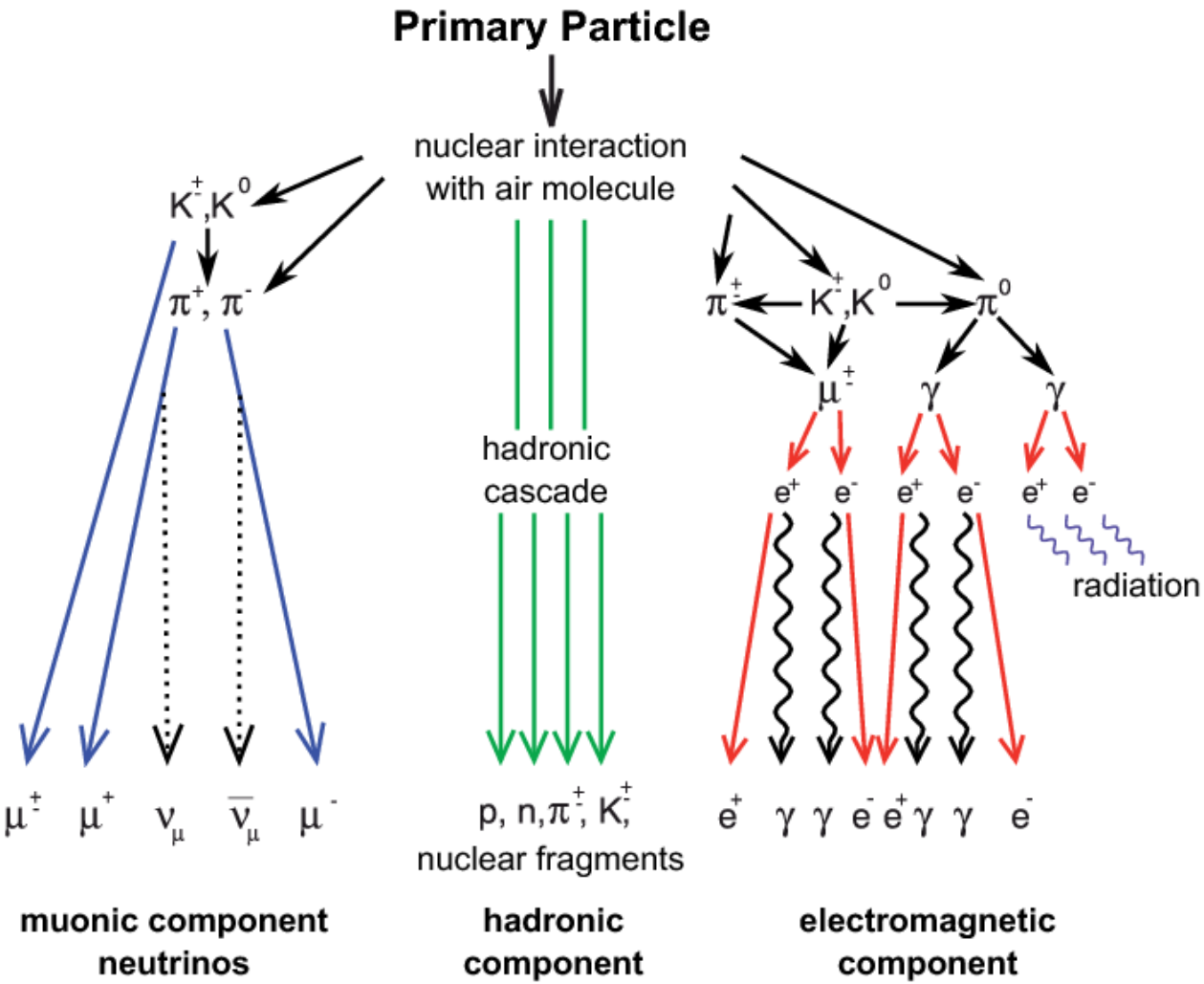

arXiv:1504.06696 [astro-ph.IM]

Extensive Air Showers: simulated shower

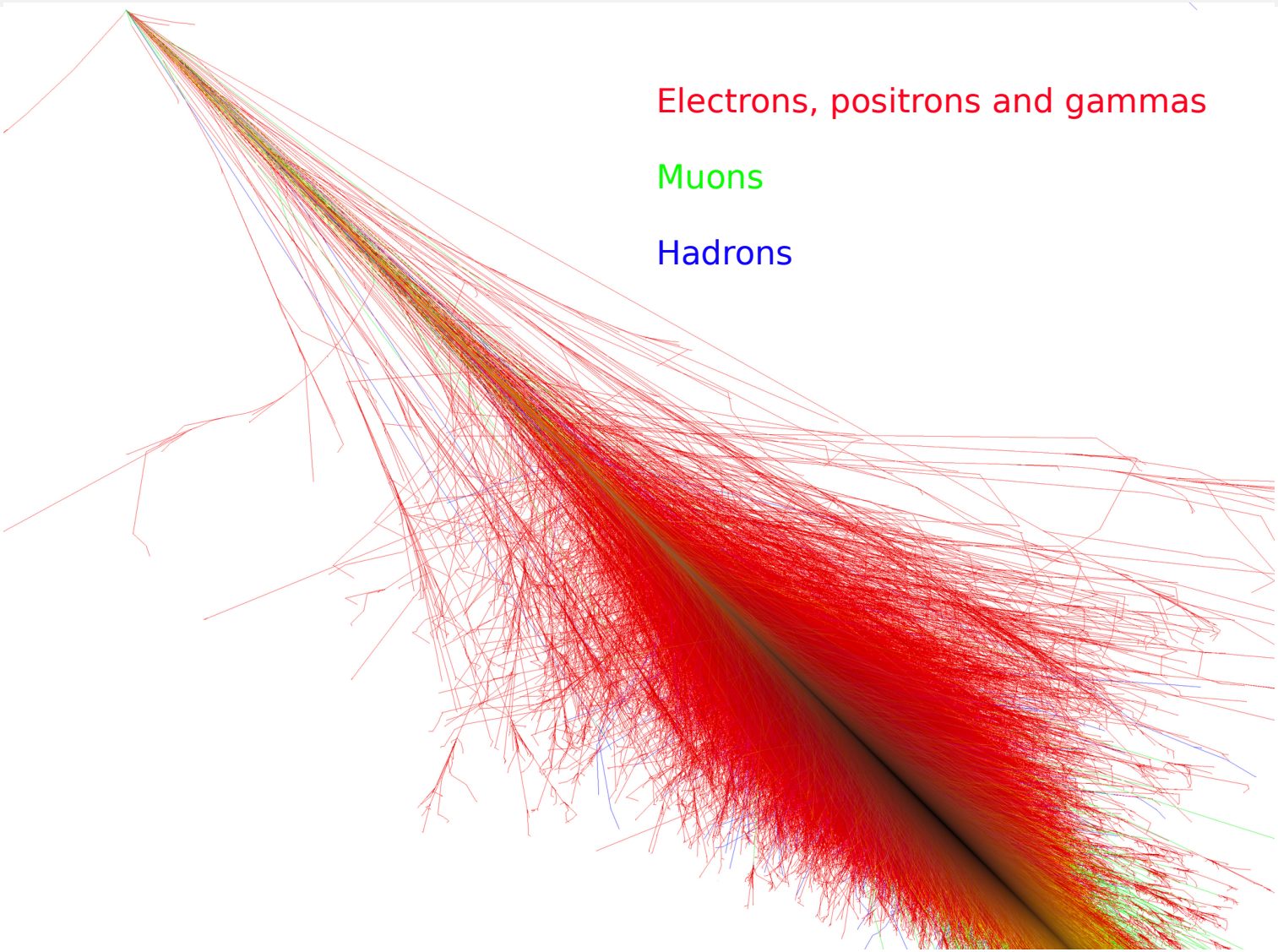

https://www-zeuthen.desy.de/∼jknapp/fs/showerimages.html

Extensive Air Shower: Longitudinal profile and X_{max}

- **Atmospheric depth:** $X(h) = \int_h^\infty \rho(l)\,\mathrm{d}l$
- **Longitudinal Profile:** Number of particles as a function of atmospheric depth X in g/cm^2
- $\boldsymbol{X_{max}}$: Atmospheric depth where the shower has the maximum number of particles
  - X_{max} depends on composition and energy of the primary particle

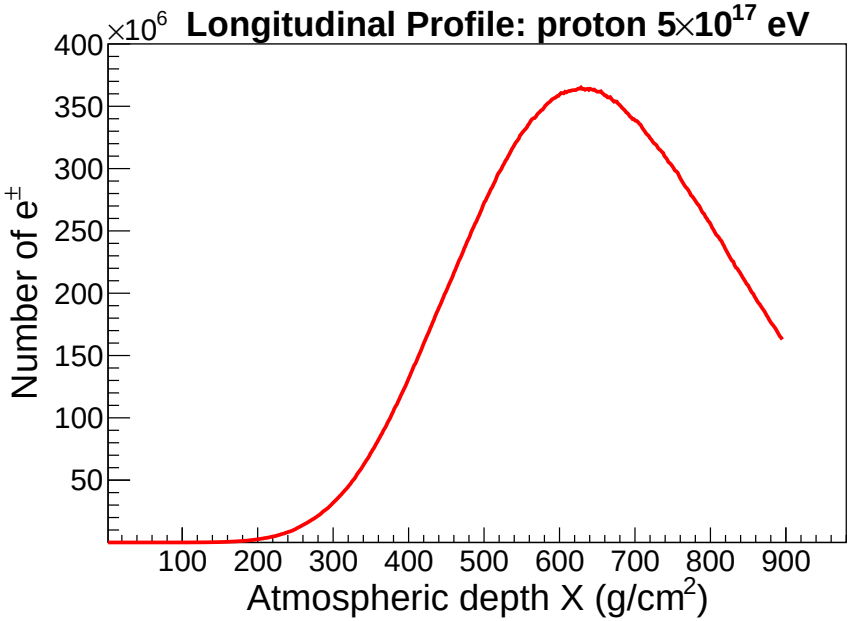

UNIVERSITY OF WARSAW

Extensive Air Showers: Heitler Toy Model EM showers

- Assumes
  - $\lambda = \lambda_{pair} \simeq \lambda_{brem}$ (mean free path)
  - Energy distributed equally between products
- After λ:
  - $\gamma \rightarrow e^+ + e^-$ (pair production)
  - $e^\pm \rightarrow e^\pm + \gamma$ (Bremmsstrahlung)

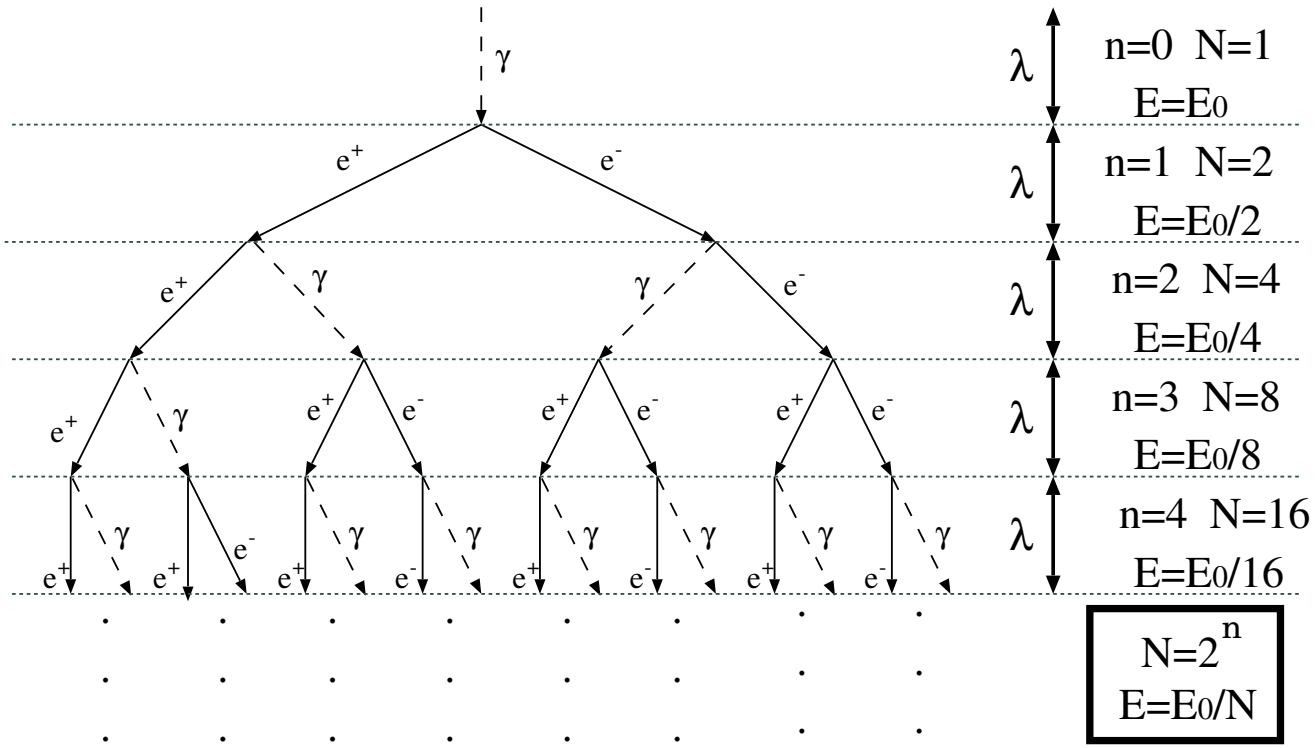

UNIVERSITY OF WARSAW

Extensive Air Showers: Heitler Toy Model EM showers

- After tranversing a distance X we have $n(X)$ generations:

$$n(X) = \frac{X}{\lambda}$$

- At this point the number of particles is:

$$N(X) = 2^n = 2^{\frac{X}{\lambda}}$$

- Each with energy:

$$E(X) = \frac{E_0}{N(X)} = \frac{E_0}{2^{\frac{X}{\lambda}}}$$

- This continues until particles reach a critical energy $E = \epsilon_c \simeq 81$ MeV in air, when they quickly loose all their energy through ionization. At this point the shower reaches its maximum number of particles:

$$E(X_{max}) = \epsilon_c = \frac{E_0}{N(X_{max})} \Rightarrow N(X_{max}) = \boxed{N_{max} = \frac{E_0}{\epsilon_c}}$$

$$E = \epsilon_c = \frac{E_0}{2^{\frac{X_{max}}{\lambda}}} \Rightarrow$$

$$\boxed{X_{max} = \lambda \log_2 \left(\frac{E_0}{\epsilon_c} \right)}$$

UNIVERSITY OF WARSAW

Superposition model

- The cascade initiated by a nucleus of mass A and energy E_0 can be approximated as a superposition of A proton showers of energy E0/A.
- The atmospheric depth of shower maximum (X_{max}) decreases as we increase the primary mass.

proton:
$$X^{p}_{max} = \lambda \log_2 \left(\frac{E_0}{\epsilon_c} \right)$$

nucleus A:
$$X^{A}_{max} = \lambda \log_2 \left(\frac{E_0/A}{\epsilon_c} \right)$$

- The heavier the primary particle, the higher up in the atmosphere the shower reaches its maximum (lower X_{max}).
- Heavy primaries have lower shower-to-shower fluctuations.
- X_{max} is as a proxy for primary composition: both $\langle X_{max} \rangle$ and $\sigma_{X_{max}}$.
- Also, N_μ increases and $N_{e^\pm}$ decreases with A (EM/hadronic ratio)

Shower EM energy dependence on primary composition

- When a UHE hadronic interaction occurs, charged and neutral pions are created (equipartition of energy): $\pi^{\pm} + X \rightarrow N\pi^{+} + N\pi^{-} + N\pi^{0}$
- The π^0 decays almost instantly into γ's, tranfering 1/3 of the energy to the EM component of the shower (γ's and $e^{\pm}$)
- There is a competition between charged pion interaction and decay:
  - If they interact, the hadronic cascade goes on and continues to feed the EM component of the shower through π^0 decay
  - If they decay, their energy turns into "missing" energy: $\pi^{\pm} \rightarrow \mu^{\pm} + \nu_{\mu}$
  - As the atmosphere is almost transparent to high energy muons, they reach the ground and their energy never feeds the EM component.
- Since a nucleus A is a superposition of lower energy showers, the pions will start with lower energies and decay earlier: smaller EM component
  - (There is a hadronic version of the Heitler toymodel, but it seems out of the scope of this talk)

UNIVERSITY OF WARSAW

Longitudinal profile: p vs Fe

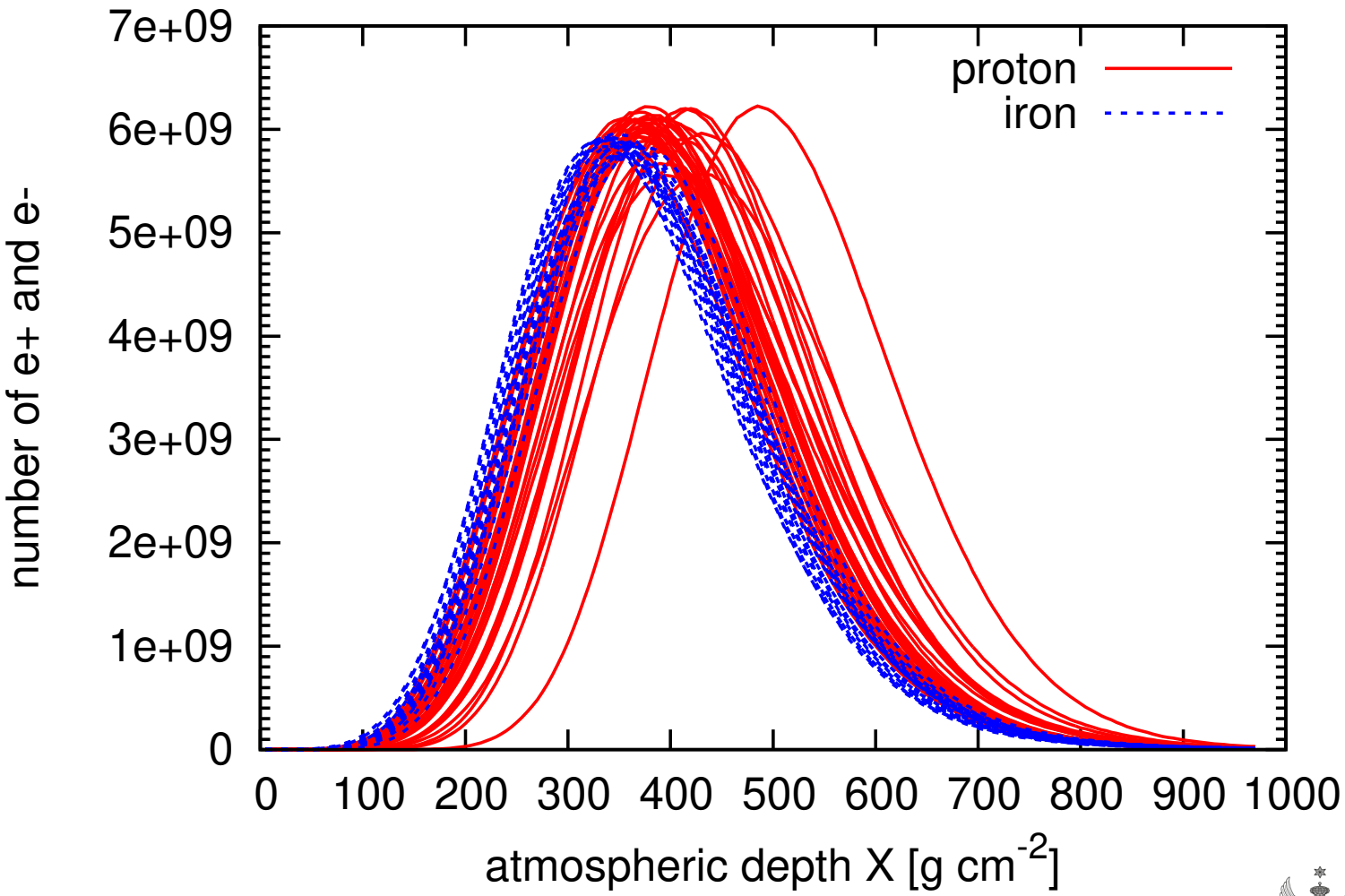

arXiv:1601.07426 [astro-ph.IM]

UNIVERSITY OF WARSAW

Detection techniques

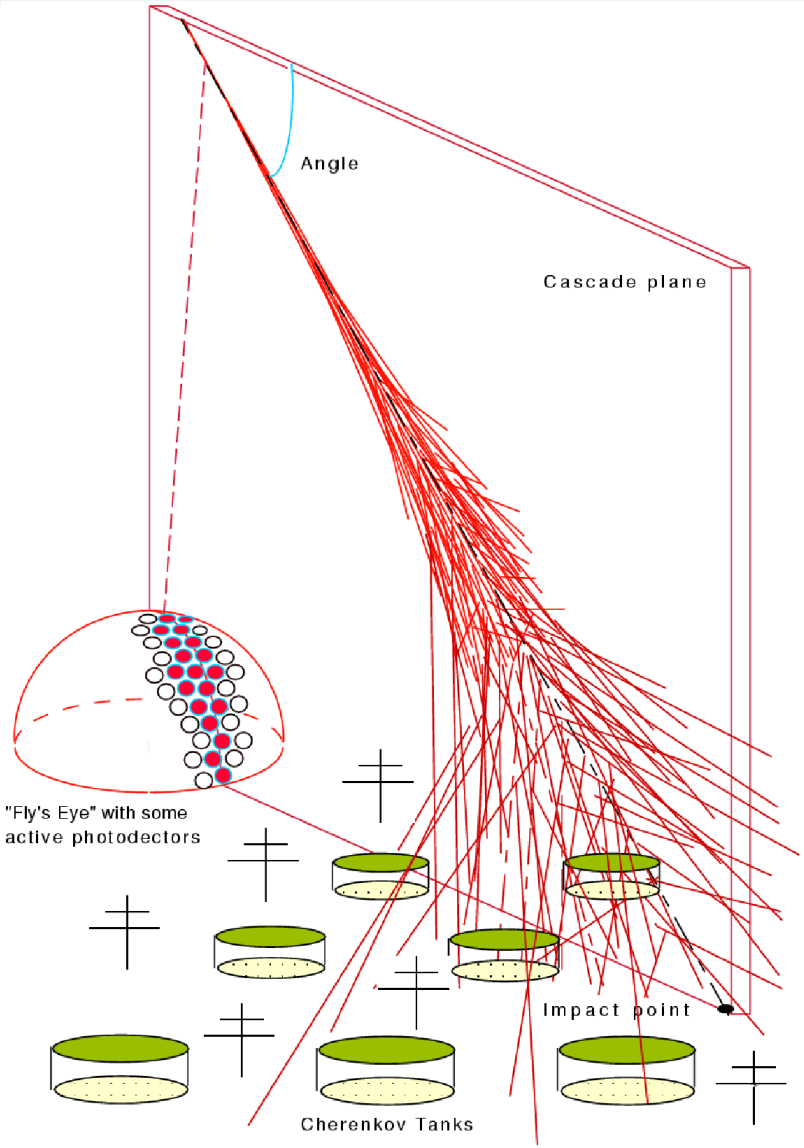

UNIVERSITY OF WARSAW

Detection techniques

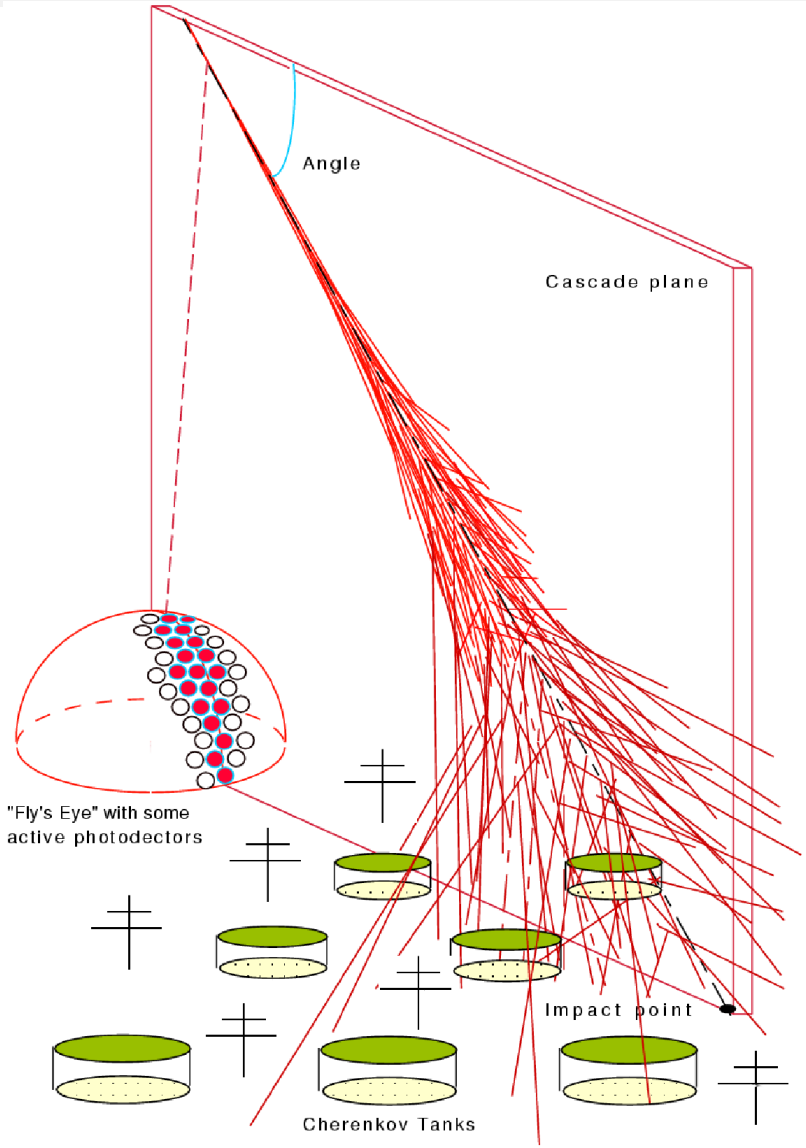

SD: Ground particles

- ☞ Measures lateral distribution at ground level
- ✓ High duty cycle
- ✗ Composition analysis very difficult
- ✓ Energy: FD calibration or simulation

UNIVERSITY OF WARSAW

Detection techniques

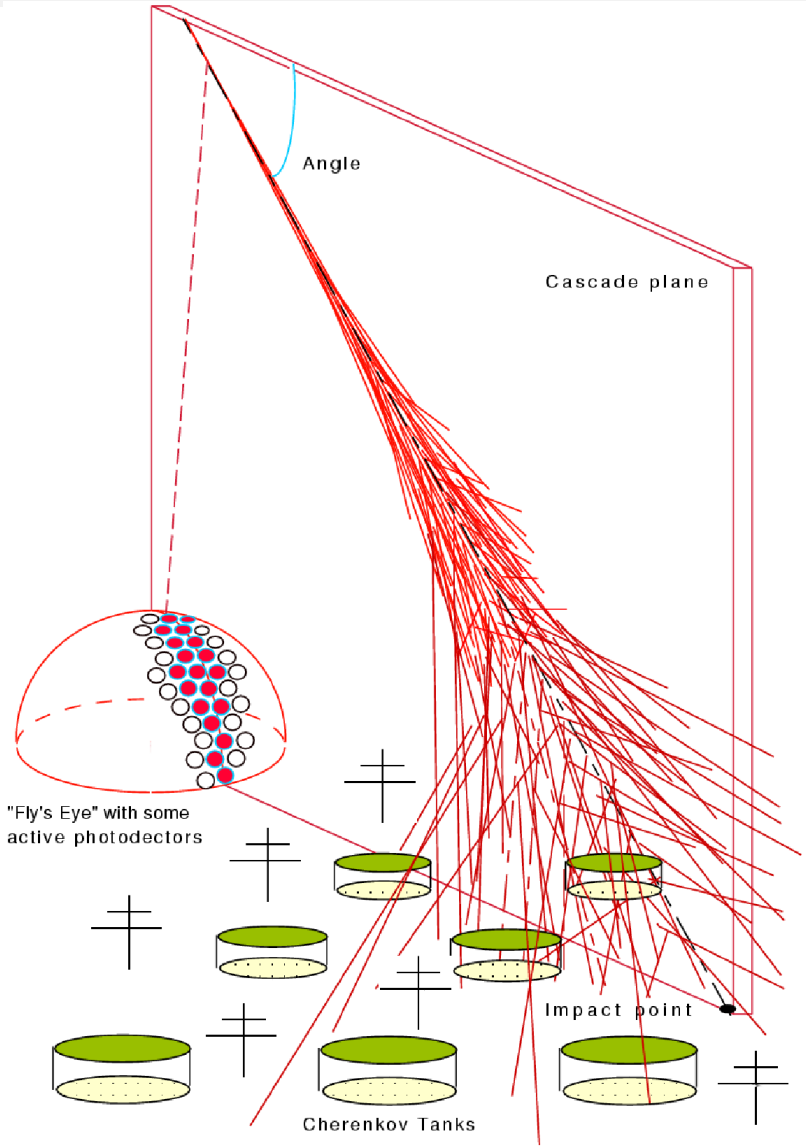

SD: Ground particles

- ☞ Measures lateral distribution at ground level
- ✓ High duty cycle
- ✗ Composition analysis very difficult
- ✓ Energy: FD calibration or simulation

FD: Shower development

- ☞ Measures the longitudinal profile ($N \times X$)
- ✗ Low duty cycle
- ✓ Composition analysis much easier (X_{max})
- ✓ Calorimetric energy measurement

UNIVERSITY OF WARSAW

Detection techniques

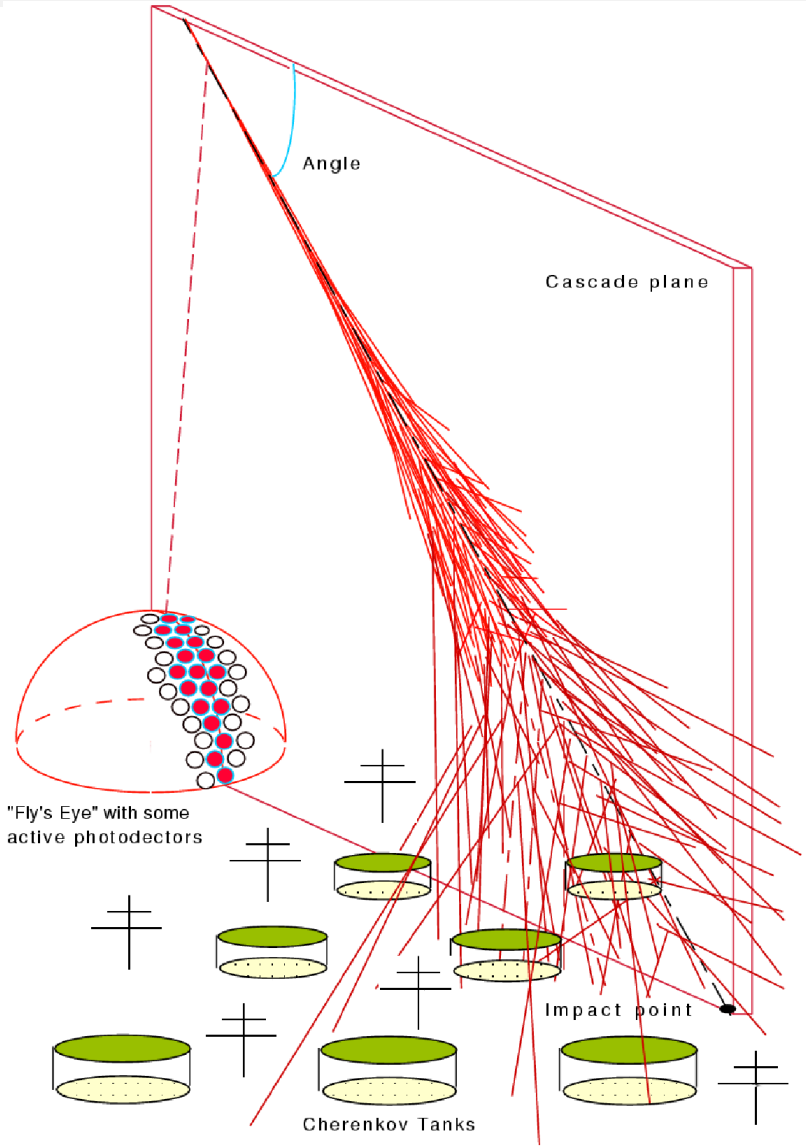

SD: Ground particles

- ☞ Measures lateral distribution at ground level
- ✓ High duty cycle
- ✗ Composition analysis very difficult
- ✓ Energy: FD calibration or simulation

FD: Shower development

- ☞ Measures the longitudinal profile ($N \times X$)
- ✗ Low duty cycle
- ✓ Composition analysis much easier (X_{max})
- ✓ Calorimetric energy measurement

Radio: EM emission of the shower

- ☞ Currently dependent on simulations
- ✓ High duty cycle
- ✓ (Almost) calorimetric energy measurement
- ✓ Sensitive to composition (X_{max})
- ✓ Lower cost

UNIVERSITY OF WARSAW

Emission mechanisms

- Two main emission mechanisms:
  - Geomagnetic emission mechanism
  - Askaryan or charge excess emission mechanism
- Moving charged particles radiate
- Movement can be described in terms of a current $\vec{J}(t)$
- From Lienard-Wiechert potentials (disregarding static term):
  - $\vec{E} \propto \frac{\partial \vec{A}}{\partial t} \propto \frac{\partial \vec{J}_\perp}{\partial t}$, where
  - $\vec{J}_\perp = -\hat{n} \times (\hat{n} \times \vec{J})$ and
  - $\hat{n}$ is the observation direction

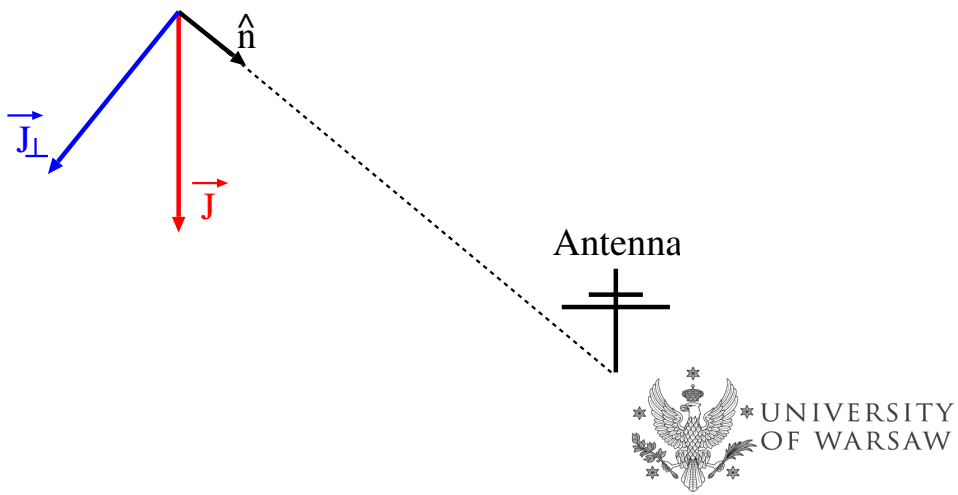

UNIVERSITY OF WARSAW

Askaryan Mechanism

- Dominates emission in dense media
- Electron and positron currents are opposite

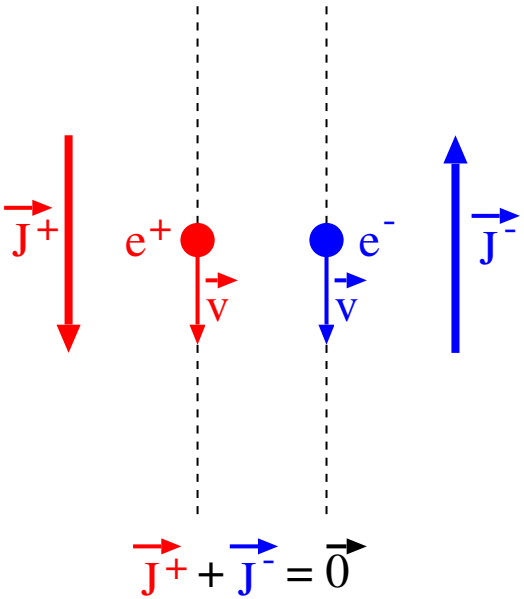

$\vec{v}$ approx. paralell to shower axis

- Emission is due to an excess of electrons in the shower
  - Shower front entrains electrons from medium

    (**Compton**, Møller, Bhabba and positron anihilation)

G.A. Askaryan, Soviet JETP 21 (1965) 658

UNIVERSITY OF WARSAW

Geomagnetic mechanism

- Dominates emission in atmospheric showers
- Charged particles deflected by geomagnetic field $\vec{B}$
- Emission from electrons and positrons add up
- The geomagnetic emission is proportional to $|\vec{B}| \sin(\alpha)$, where α is the angle between the shower axis and $\vec{B}$

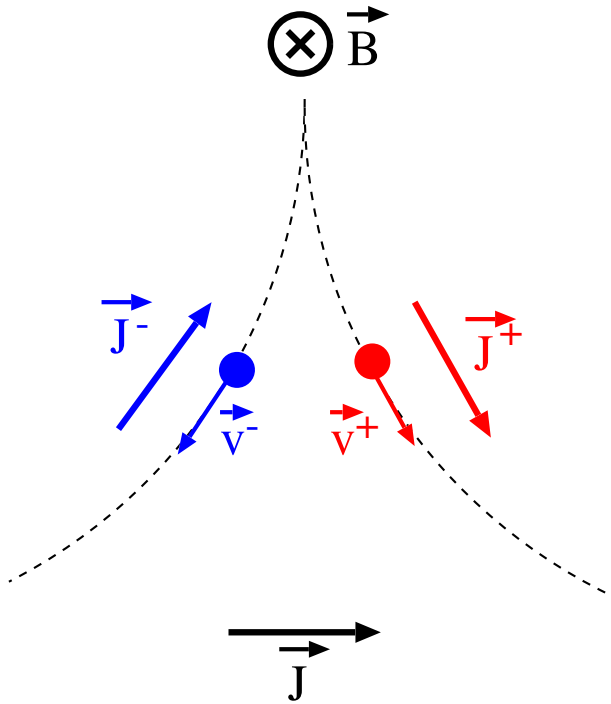

F.D. Kahn and I. Lerche, Procs. Royal Society A 289 (1966) 206

UNIVERSITY OF WARSAW

Polarization

- **Geomagnetic mechanism polarization ($\vec{G}$)**
  - Aproximatelly paralell to $-\vec{V} \times \vec{B}$
  - Independant of observer position
- **Askaryan mechanism polarization ($\vec{A}$)**
  - Aproximatelly radial w.r.t. shower axis $\vec{V}$
  - Depends on observer position
- The superposition of these two polarizations will make the radio footprint at ground level asymmetric

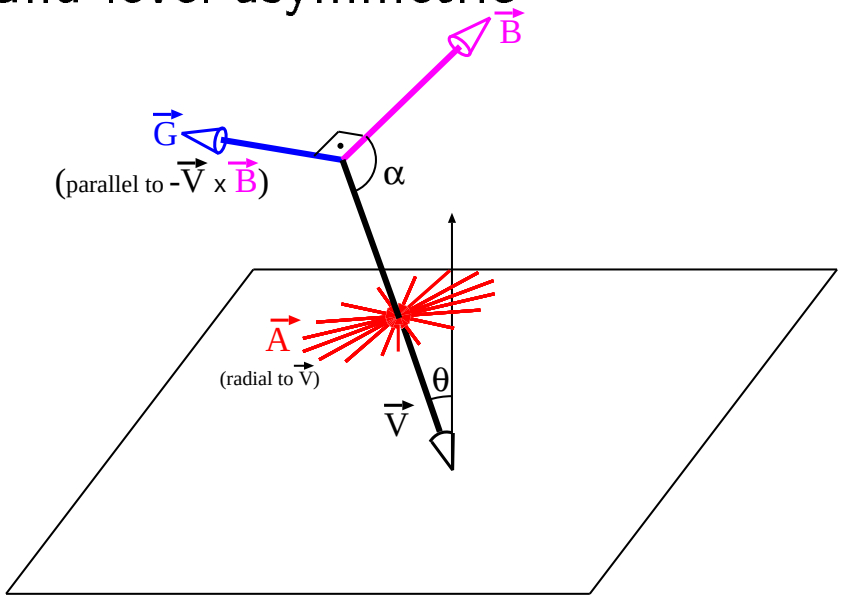

UNIVERSITY OF WARSAW

Cherenkov-like effects

Relativistic effects play crucial role in emission

- Stem from atmospheric refractive index $n > 1$ (n=1.000325 @ sea level)
- Shower front travels faster than emission
- Time reversal / multiple parts of EAS seen simultaneously
- Large "time compression" around part seen at $\theta_C = cos^{-1}(1/n)$
- Different antennas are more sensitive to different parts of the shower

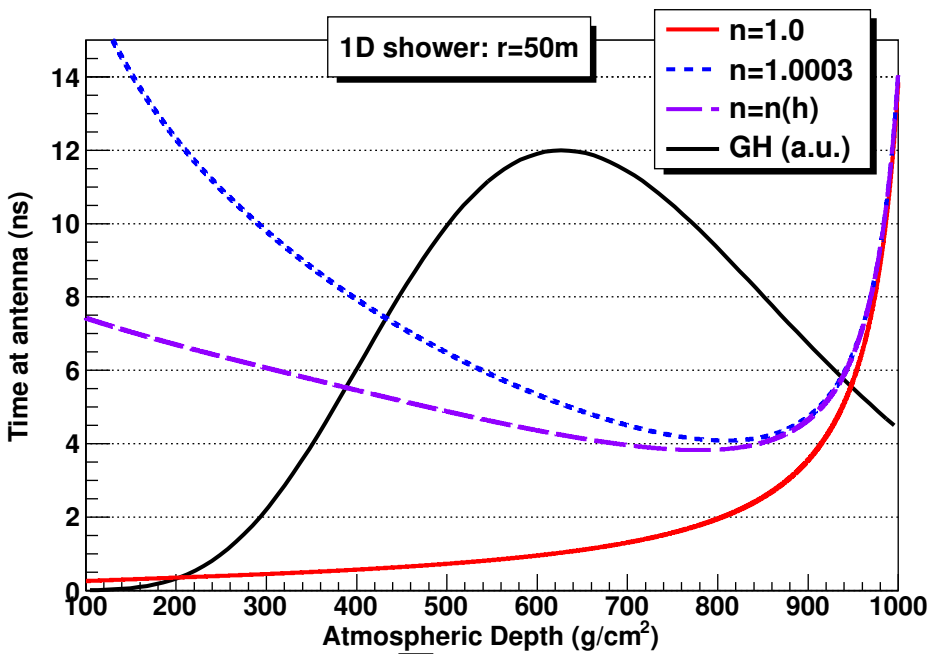

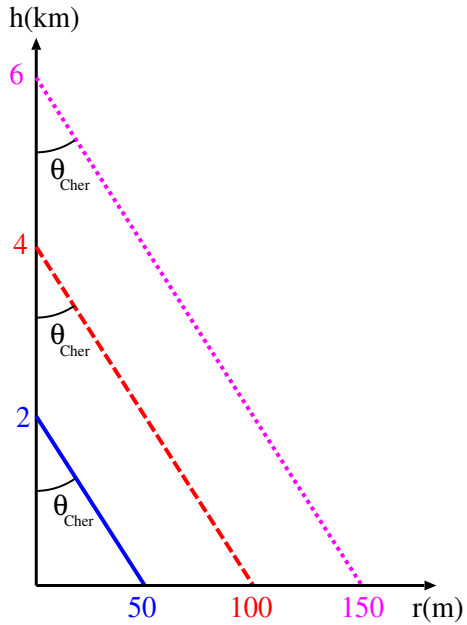

Santiago group, Astropar.Phys., **35**, (2012) 325

Cherenkov Ring

Observers that see X_{max} at θ_C

- Define a ring-like region on the ground
- Maximum field amplitude
- Sizeable intensity well into the GHz range
- Ring is elliptical for non-vertical showers

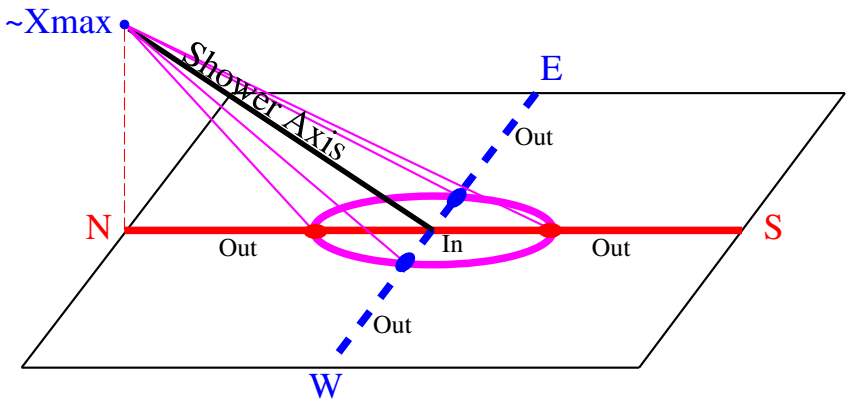

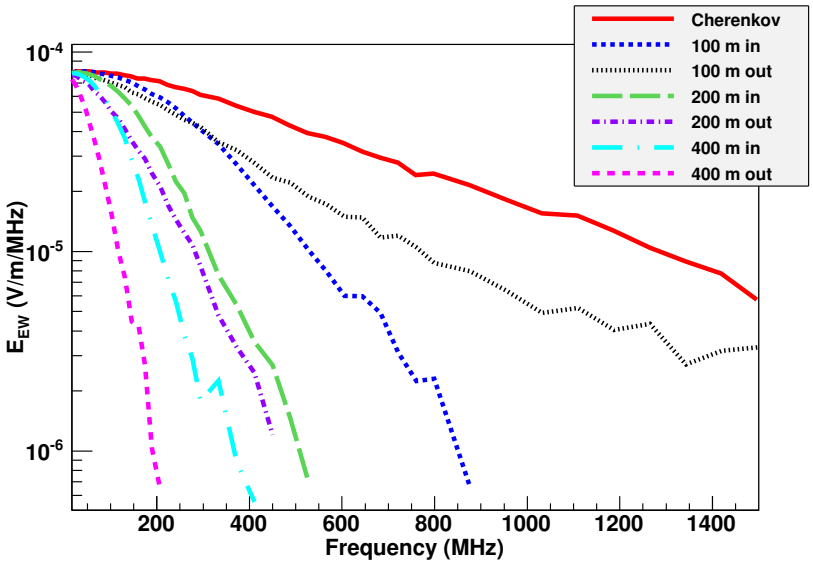

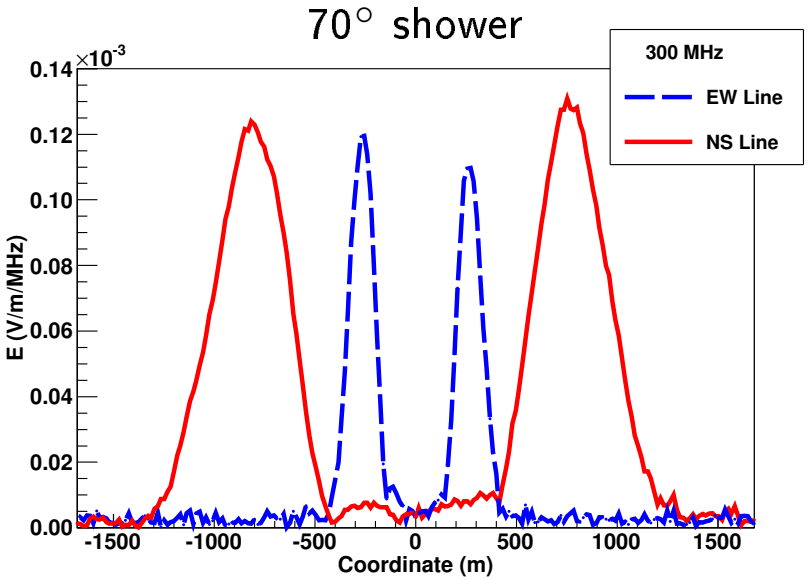

J. Alvarez-Muñiz, W. Carvalho Jr., A. Romero-Wolf, M. Tueros, E. Zas, Phys. Rev. **D 86** (2012) 123007

Shower geometry: Zenith, X_{max} position and footprint size

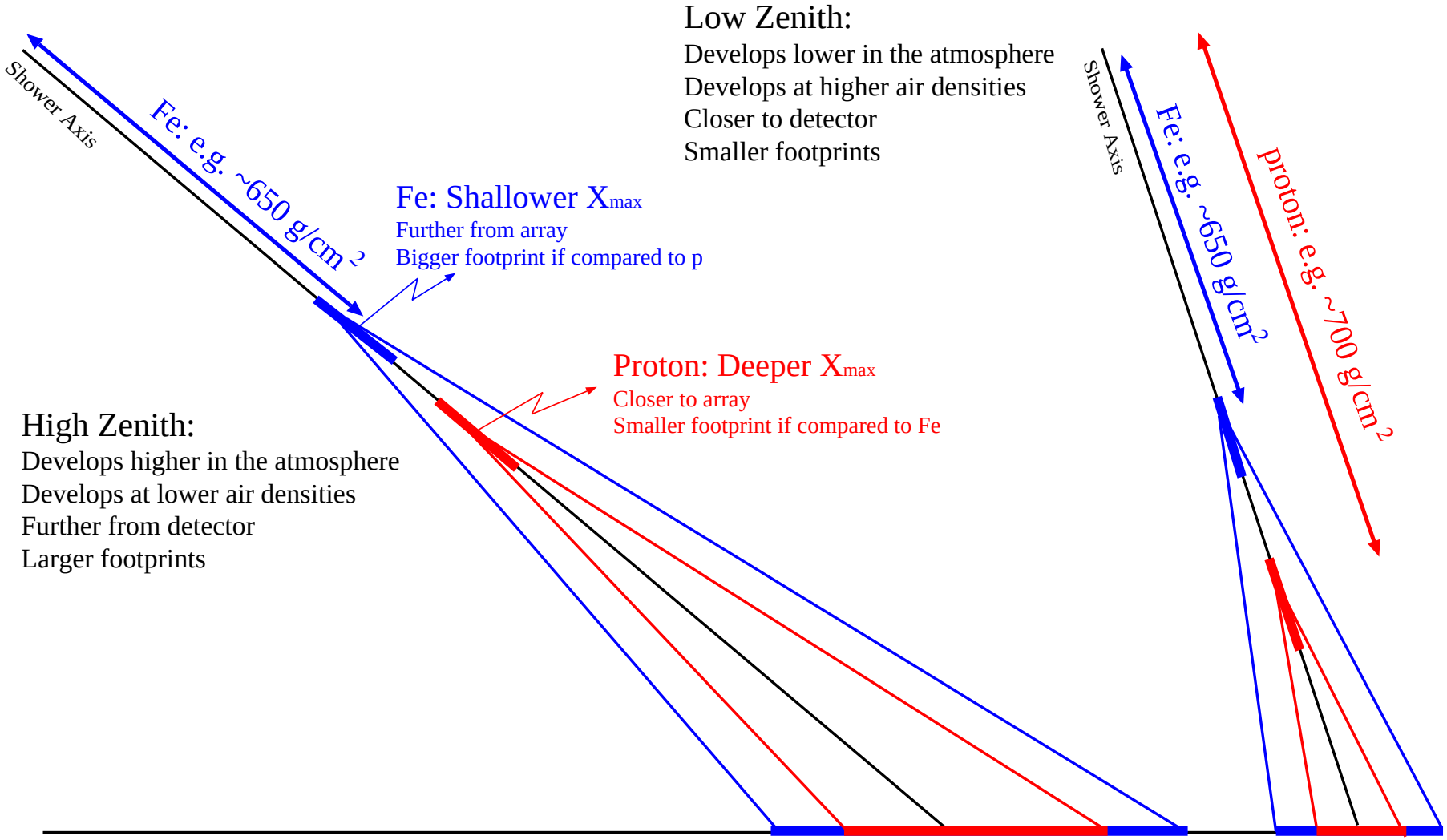

Radio footprint at ground

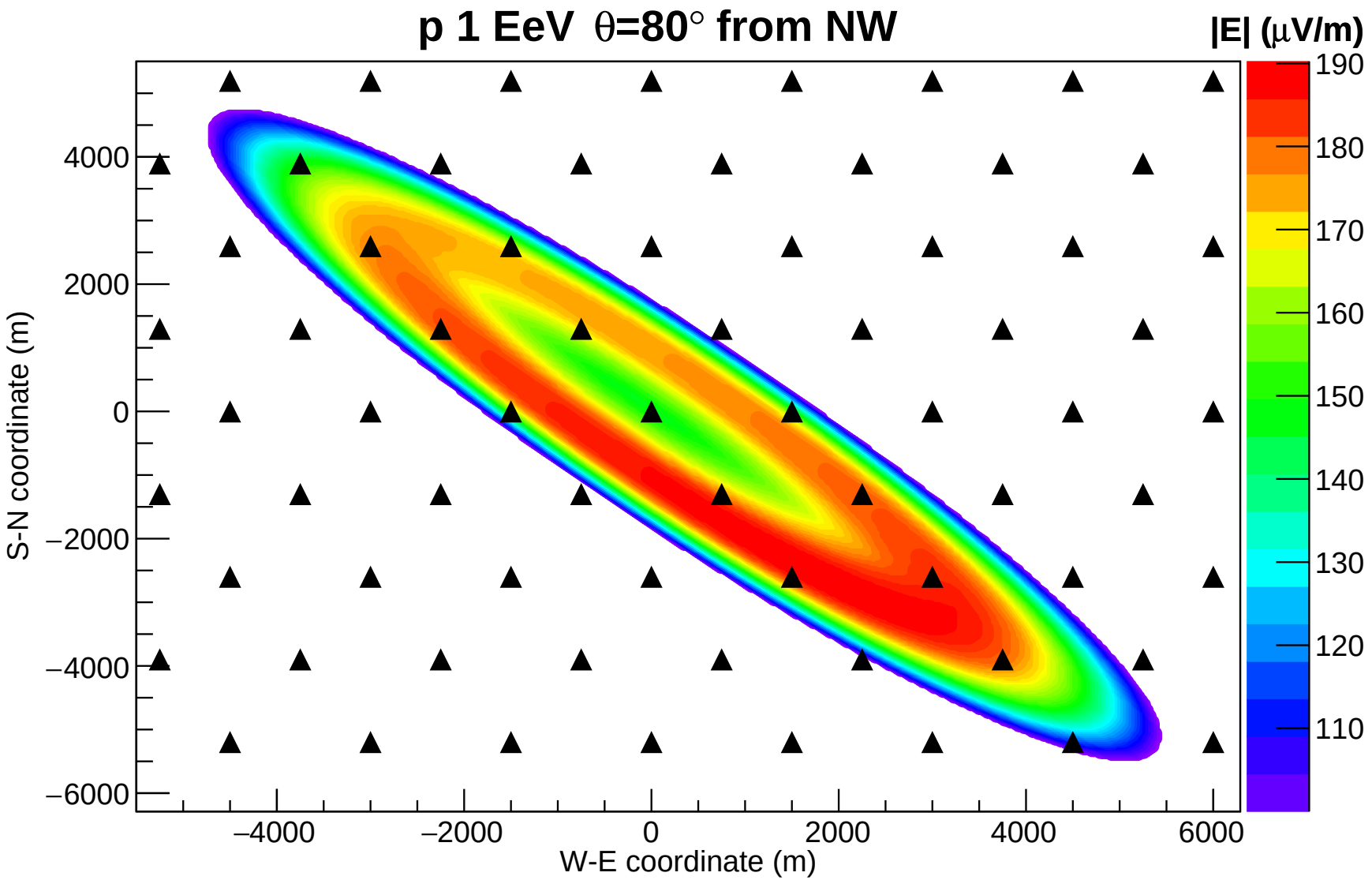

Lateral Distribution Function (LDF)

"Peak amplitude as a function of distance to the core"
(Along a line of antennas on a single direction for this seminar)

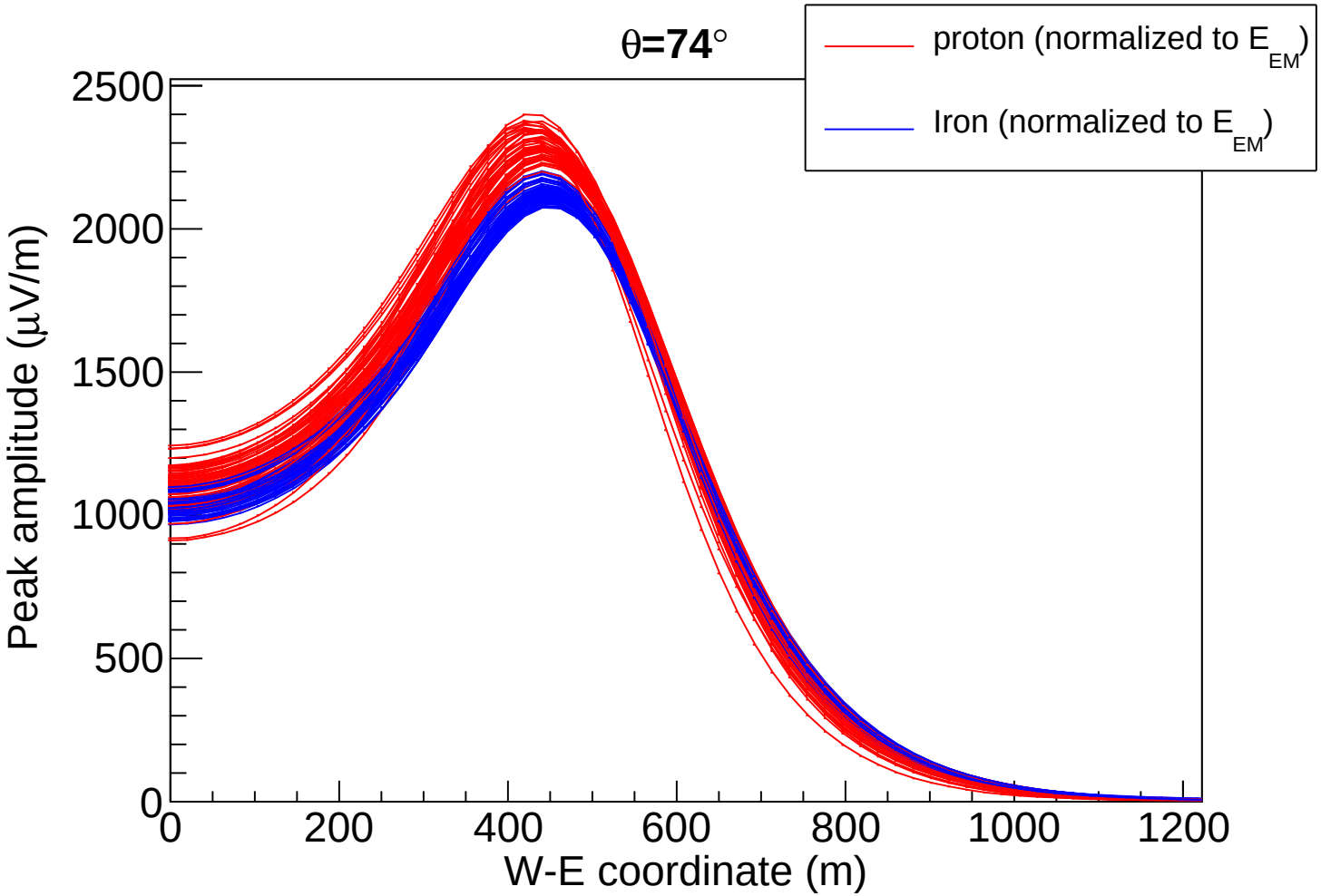

Simulation of the radio emission: ZHAireS

- AIRES: Full shower simulation
  - Well known and widely used EAS simulation software
  - Microscopic approach
  - All relevant EM and hadronic processes taken into account
  - Propagates shower particles (interactions, decays, deflections, etc..)
  - Gives access to every charged particle track in the shower
- ZHAireS (ZHS + AIRES): Radio emission addon to AIRES
  - Uses ZHS formalism (**Z**as, **H**alzen and **S**tanev) to calculate emission
  - Algorithm based on first principles
  - Does not pressuppose any emission mechanism
  - Calculates the contribution of every particle track to the radio emission

UNIVERSITY OF WARSAW

ZHS: Algorithm for $\vec{A}$ calculation

- Vector potential equation: Radiation from a single finite particle track

$$\vec{A}(t,\hat{u}) = \frac{\mu e}{4\pi R c}\vec{\beta}_{\perp}\frac{\Theta(t-t_1^{det})-\Theta(t-t_2^{det})}{1-n\vec{\beta}\cdot\hat{u}},$$

$$\vec{E}(t) = -\frac{\partial\vec{A}}{\partial t}$$

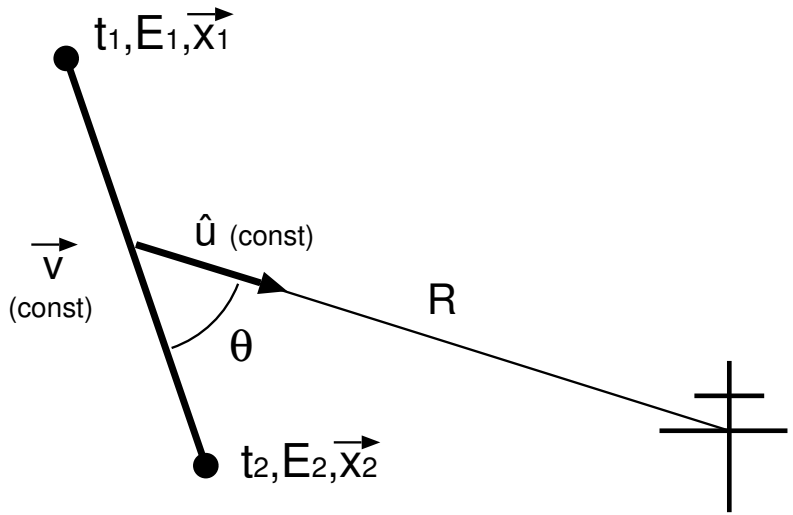

(Phys.Rev.D81:123009,2010)

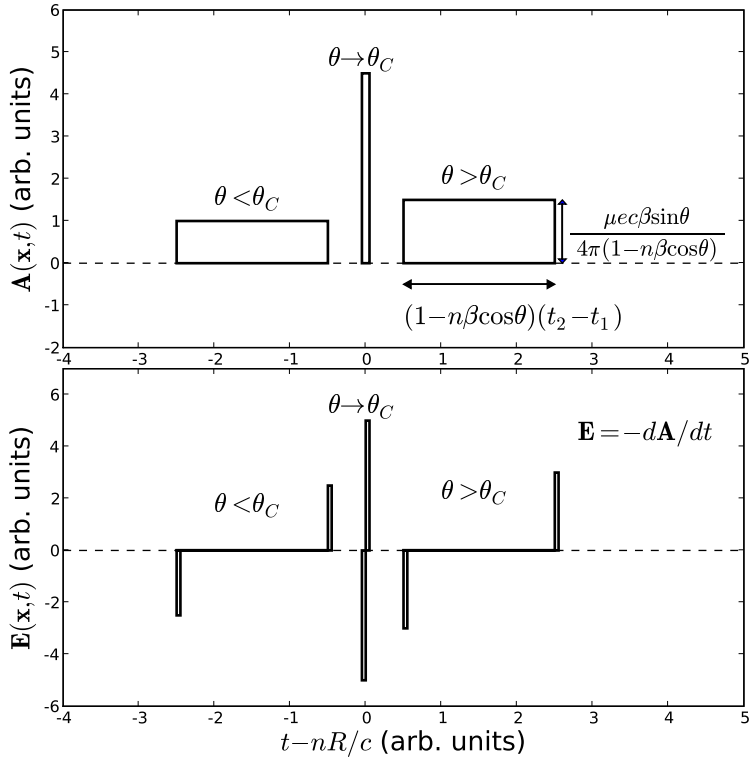

Section 2

Revisiting the radio LDF dependence on CR primary composition

Why did I revisit the Radio LDF? ML discrimination

- We developed a Machine Learning (ML) Random Forest algorithm that discriminates between heavy (Fe) and ligth (p) primary compositions on an event-by-event basis
- Bypasses any X_{max} reconstruction and infers composition directly
- Similar to a previous approach: Astropart.Phys **109**, 41-49, 2019
  - Comparisons to simulations, similar to LOFAR X_{max} method (χ^2)
  - But infers composition directly, bypassing any X_{max} reconstruction
- Good accuracies in general even with a huge 30% energy smearing
- Input: Event simulations on GP300 (GRAND prototype). Just used the antenna distances to the axis and the peak field amplitudes
- Random Forest is not a black-box!
  - We analysed the feature importances to understand what is relevant for the discrimination
  - Proton showers seemed to be brighter than Fe near the core

Random Forest Features

- Triggered antennas are ordered with increasing distance to the axis
- For each antenna i we used:
  - The distance d_{Ai} to the shower axis and the peak amplitude $|E_i|$
  - Features: $d_{A1}, |E_1|, d_{A2}, |E_2|, ..., d_{Ai}, |E_i|$
  - The number of features is $2\times$ the number of antennas triggered by the event with the most antennas
  - For events with less antennas, missing features are subtituted by zeros
  - Primary composition also saved (p or Fe)

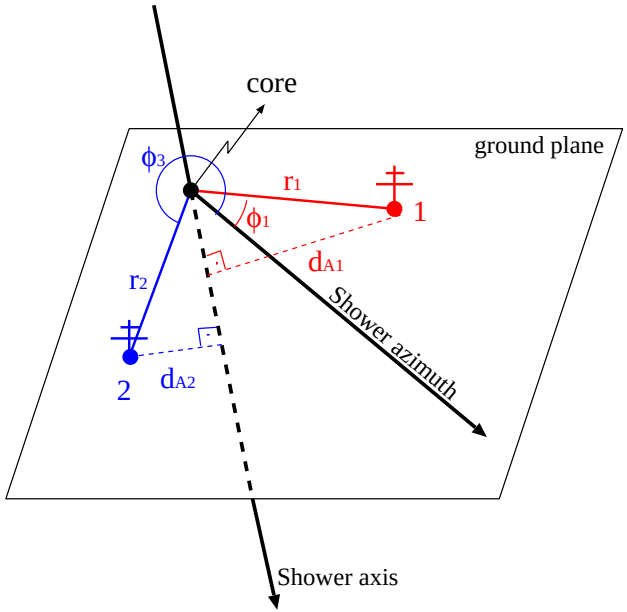

UNIVERSITY OF WARSAW

Discrimination accuracy with hexagonal arrays

- To simplify the analysis, we applied the same method to single antenna distance hexagonal arrays instead of the (asymmetric) GP300 array
- We scaled each shower by its own EM energy
  - Takes into account EM energy differences between p and Fe
  - All showers now have the exact same EM energy
- We also decreased the energy smearing to 10% (now EM energy only)
  - EM energy uncertainty is estimated as <5%: JCAP01(2023)008

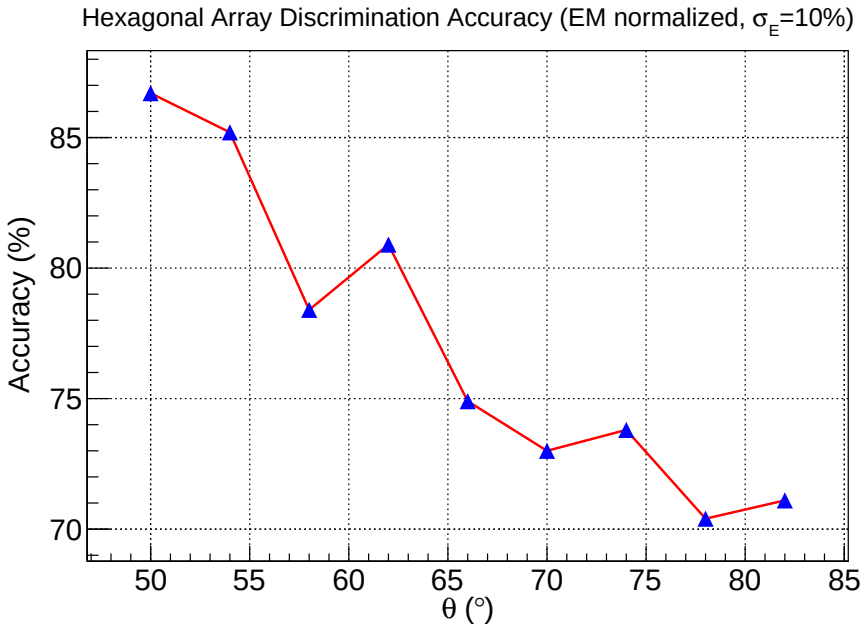

Hints from parameter importances

- Random Forest $\theta = 62°$ GP300
- Discrimination accuracy: $\geq 73.3\%$ (Not fully optimized yet)
- Most important feature: Amplitude of closest antenna followed by antennas after the Cherenkov ring
- This hints at protons being brighter near the core!

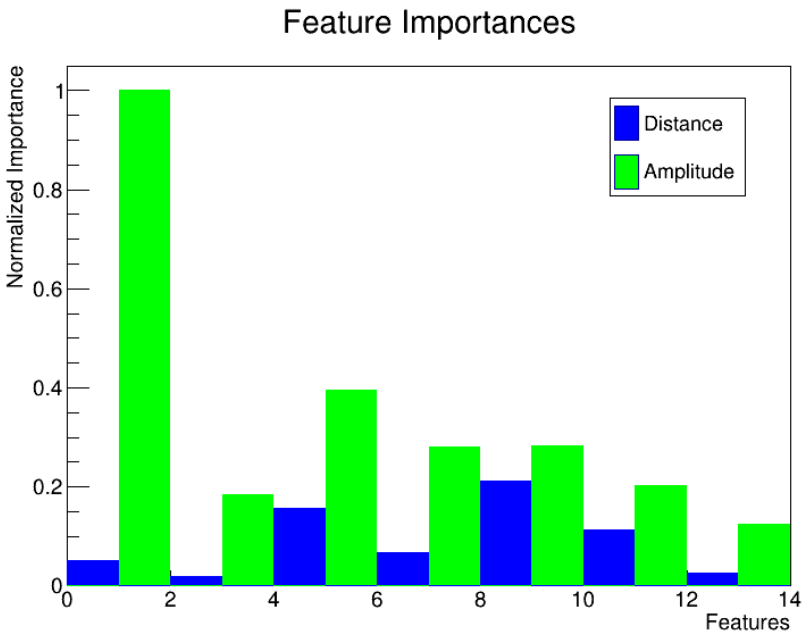

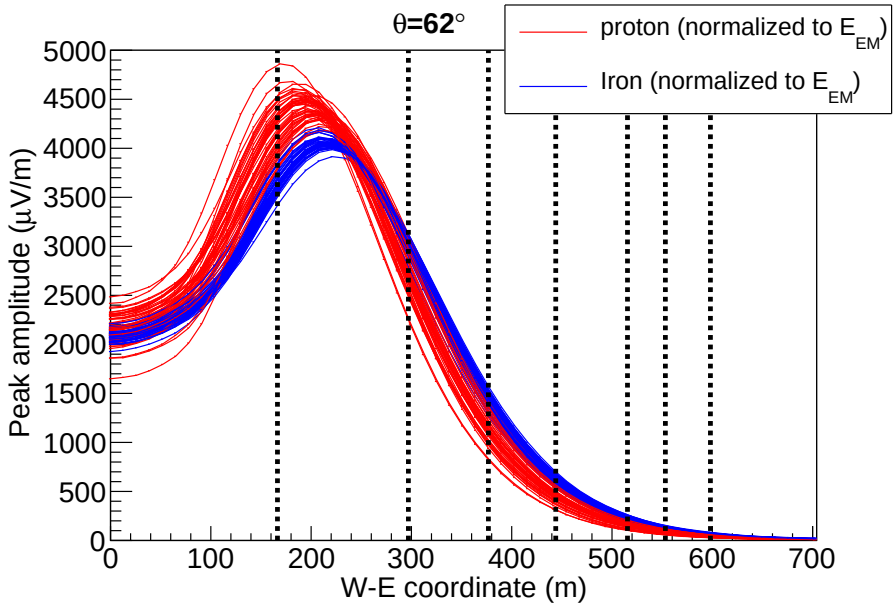

Radio footprint depends on X_{max} and composition

- It is well known that X_{max} changes the radio footprint on the ground
- Basis of many analyses, e.g., LOFAR-like X_{max} reconstructions
  - Based on comparisons of data with multiple simulations
  - Similar to a χ^2 analysis: It is a "Black Box"
  - People stopped looking at plots of the LDF for different compositions!

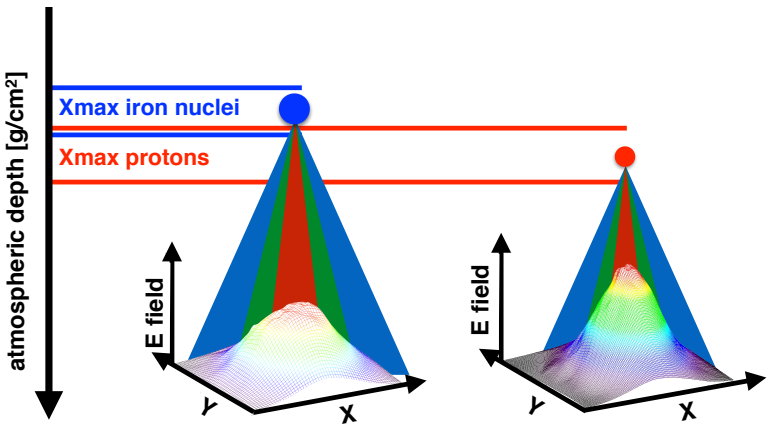

S. Buitink, et al., arXiv:1408.7001 (2014)

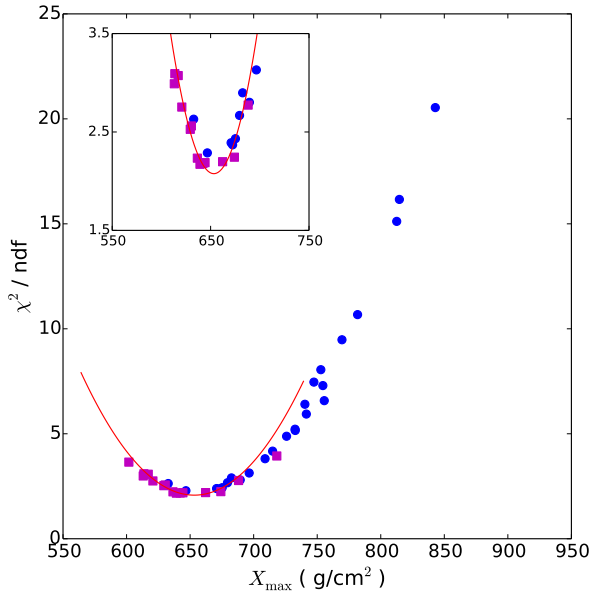

Florian Gaté, arXiv:1609.06510 (2016)

Earlier method: LDF slope (LOPES and Tunka-Rex)

- Slope of the meausred LDF at a certain distance correlated to X_{max}
- Used before the LOFAR-like X_{max} reconstruction for low zenith events
- At that time people actually looked at LDF plots for multiple compositions and multiple X_{max}
- This stopped after the introduction of the LOFAR method (Black box)

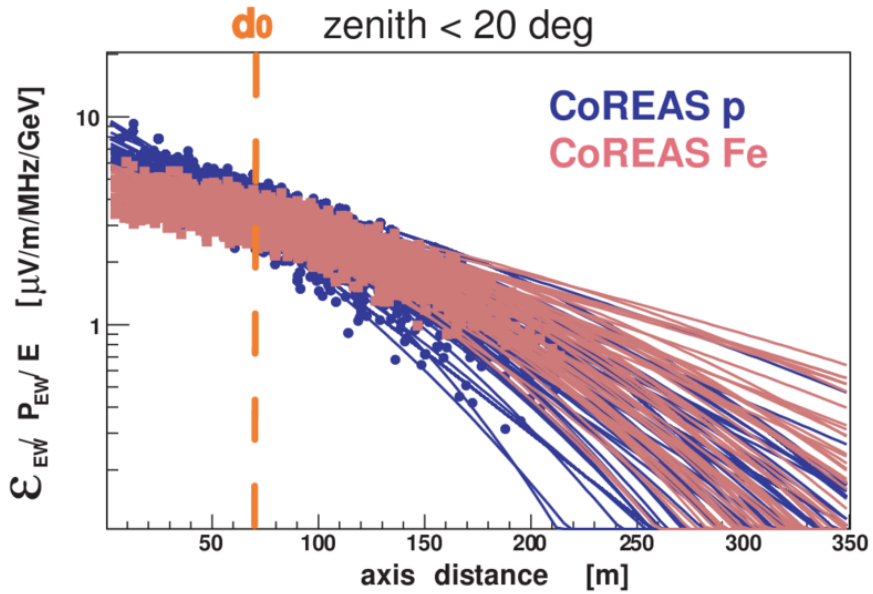

N. Palmieri, et al. (LOPES), arXiv:1309.2410 (2013)

UNIVERSITY OF WARSAW

Full ZHAireS simulations

- We used full ZHAireS simulations to obtain the radio emission
- Antennas on a single line East of the core (no asymmetry!)
- 50 p and 50 Fe showers per zenith angle
- Electric fields normalized by the EM energy of each shower
  - Removes effects due to missing energy differences between p and Fe
    - At 1.25 EeV, on average, $\sim 10\%$ for p and $\sim 15\%$ for Fe
- 2 sites: GRAND and AUGER
- GRAND:
  - Ground at 1264 m, $|B| = 56.4 \mu T$, 50-200 MHz
  - Showers with $E_0 = 1.25$ EeV coming from the North
  - Zeniths between 42 and 82° in steps of 4°
- AUGER (older simulation set):
  - Ground at 1400 m, $|B| = 24.0 \mu T$, 30-80 MHz
  - Showers with $E_0 = 5$ EeV coming from the South
  - Zeniths between 55 and 85° in steps of 5°

UNIVERSITY OF WARSAW

How does the radio LDF actually looks like?

- This type of composition dependence was already seen before
- But was never fully pursued
- Mostly dismissed as just a missing energy effect
- But it is much more than that!

First comparison between CoREas, ZHAireS and AERA data (ca. 2013):

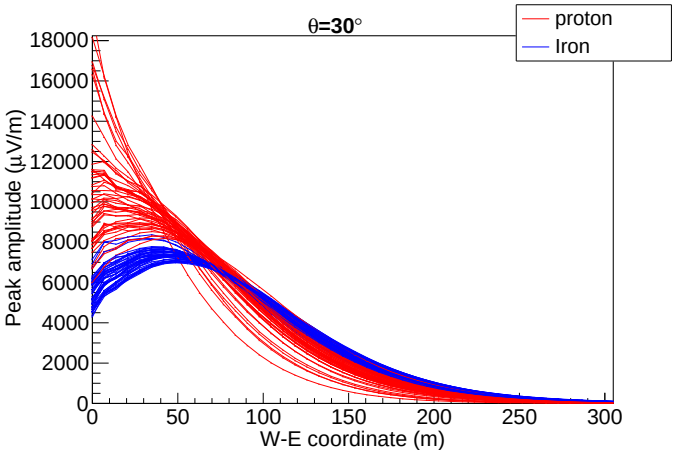

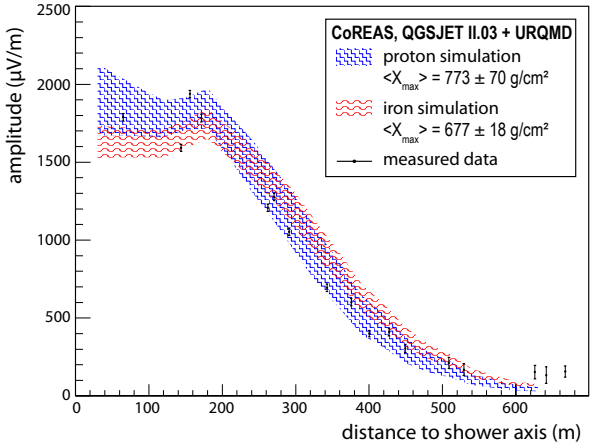

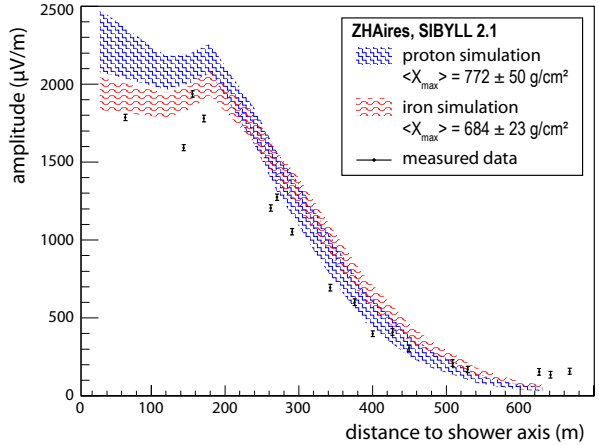

This work (Not same zenith or E0)

Tim Huegue, arXiv:1310.6927

UNIVERSITY OF WARSAW

How does the radio LDF actually looks like?

- But the old LDF slope method for low zenith was onto something!

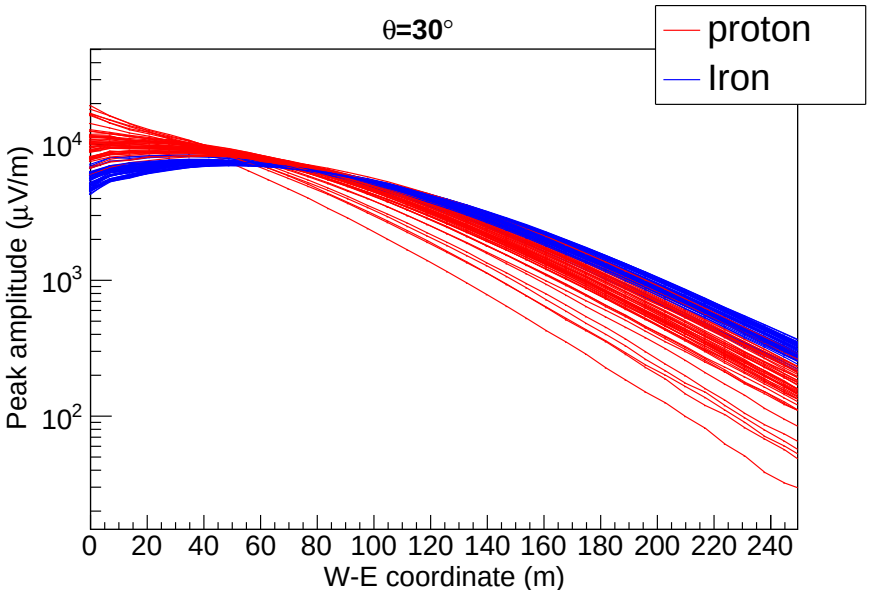

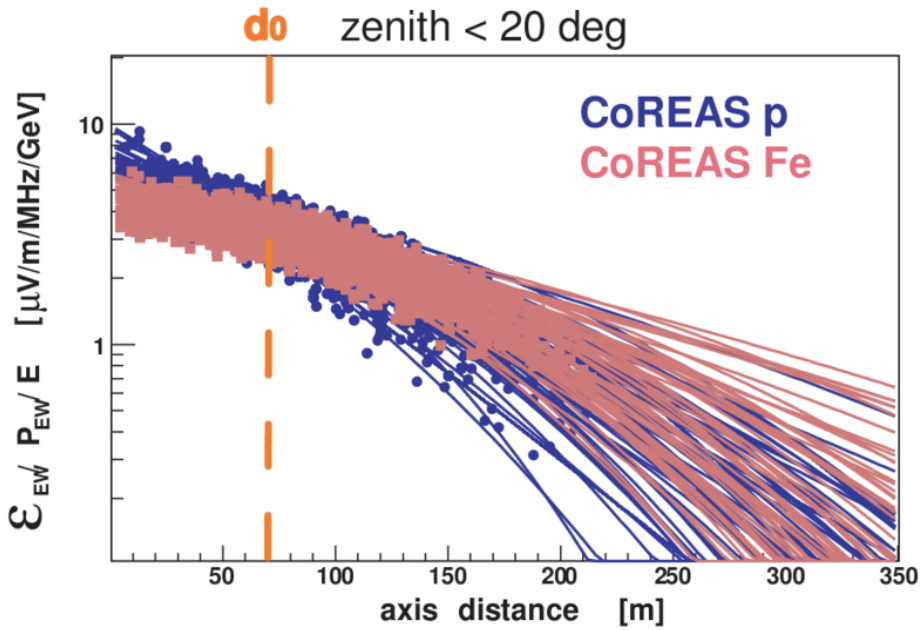

How does the radio LDF actually look like?

- Composition (X_{max}) dependence much bigger than missing energy (EM energy) differences between p and Fe
- Normalizing the fields by the EM energy of each shower makes this dependence even more clear and well behaved
- Now all showers have the same EM energy (Not E_0)
- Protons indeed have higher fields near the core at GRAND!

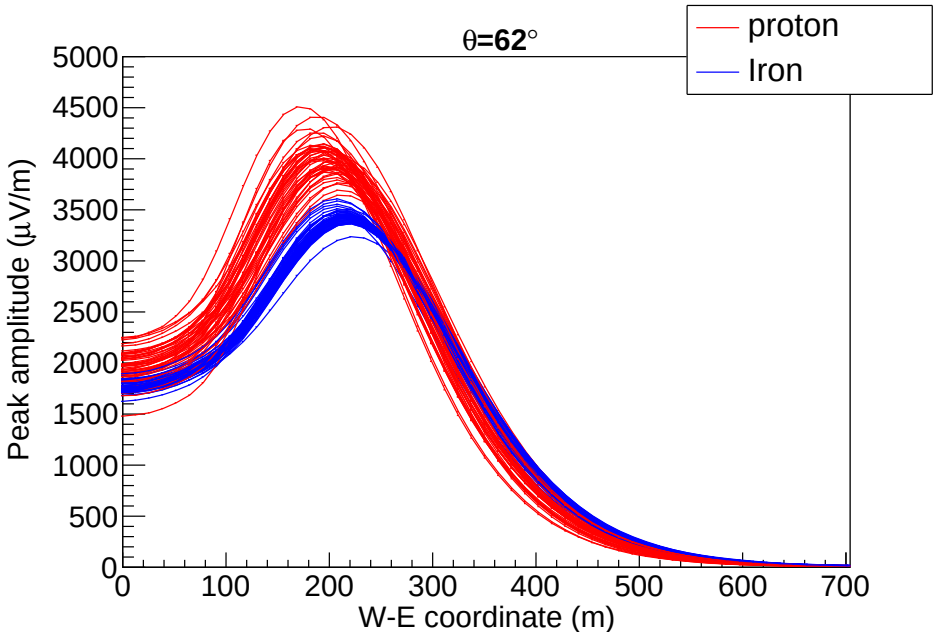

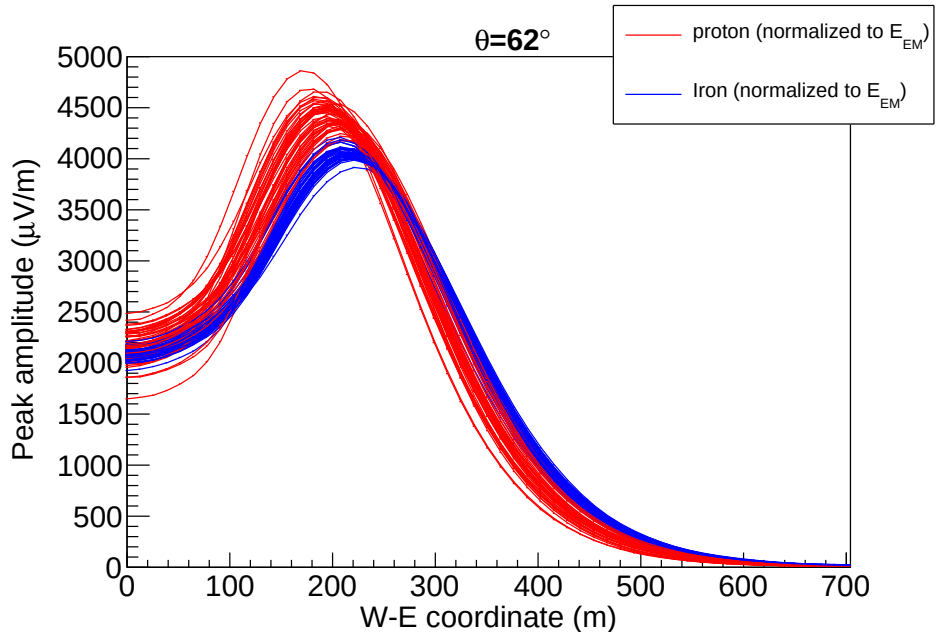

Radio LDF higly affected by zenith angle

GRAND

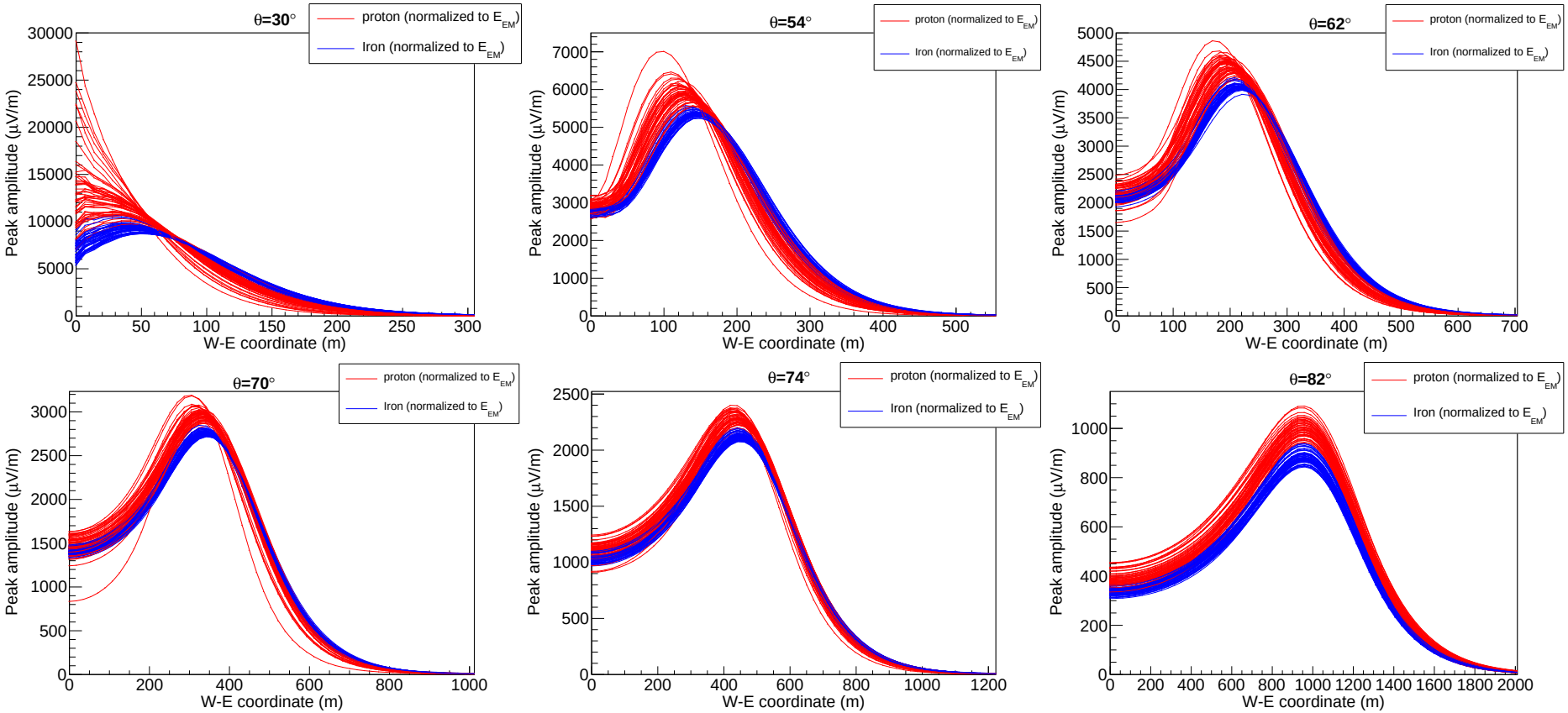

The "Magic angle" ($\sim 84°$)

- Near the "Magic angle" $\sim 84°$:
  - The footprint size decrease due to a decreasing θ_{Cher} with altitude cancels out the size increase due to the larger distances (projection)
  - Around this angle the radio footprint shape (illuminated area, ring position) does not depend on X_{max} anymore.
  - Footprint shape is the same regardless of X_{max} , but the amplitude still depends on X_{max} (composition)

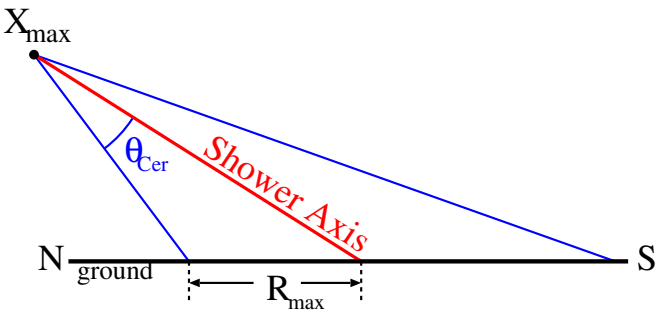

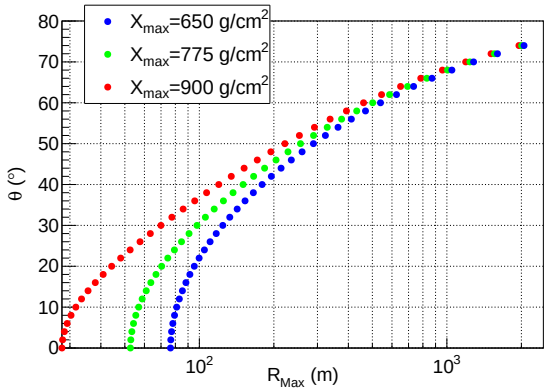

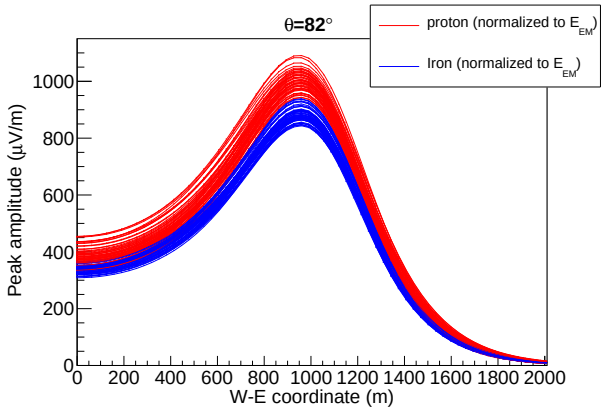

W. Carvalho and J. ALvarez-Muñiz, arXiv:1712.03544

UNIVERSITY OF WARSAW

Peak electric field amplitudes

- Peak amplitudes (normalized by EM energy) for the GRAND simulation set as a function of zenith angle
- Protons tend to have higher peak electric fields at every zenith angle

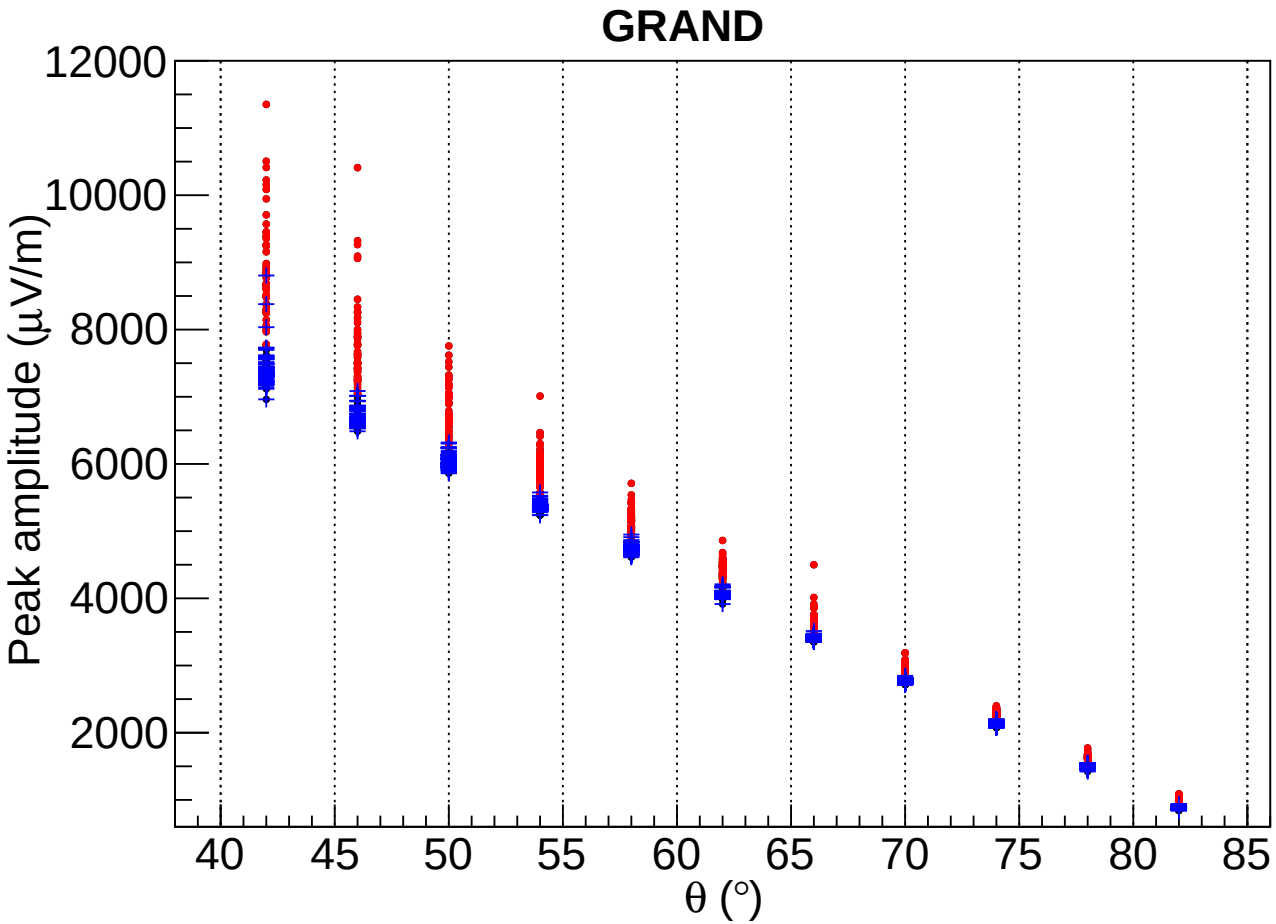

Peak electric field amplitudes

- Peak amplitudes (normalized by EM energy) for the GRAND simulation set as a function of the density ρ at X_{max}
- Amplitude differences between p and Fe diminish at lower ρ (higher θ)
- This decreases the discrimination accuracy with increasing zenith

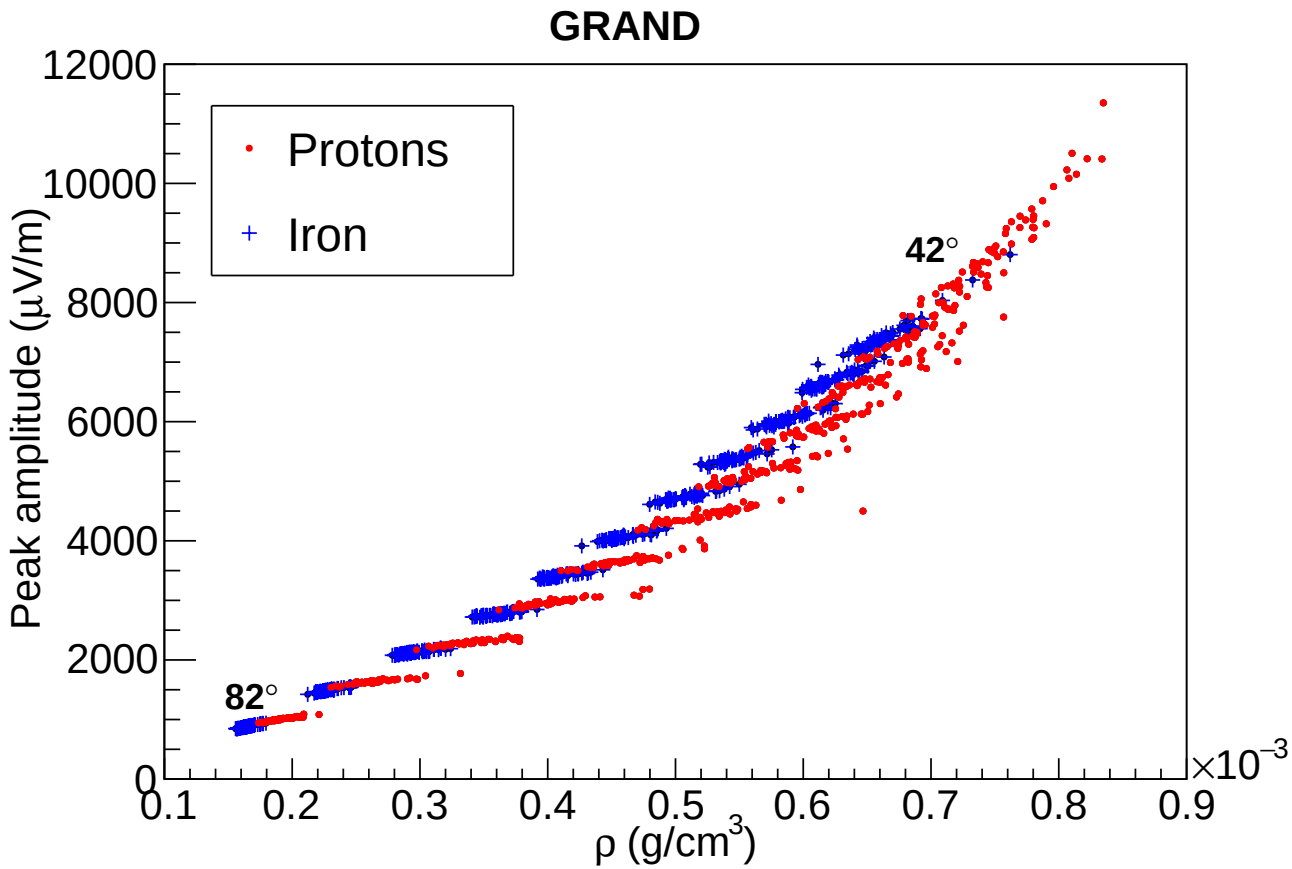

UNIVERSITY OF WARSAW

Peak electric field amplitudes

- Peak amplitudes (normalized by EM energy) for the GRAND simulation set as a function of the density ρ at X_{max}
- Amplitude differences between p and Fe diminish at lower ρ (higher θ)
- This decreases the discrimination accuracy with increasing zenith

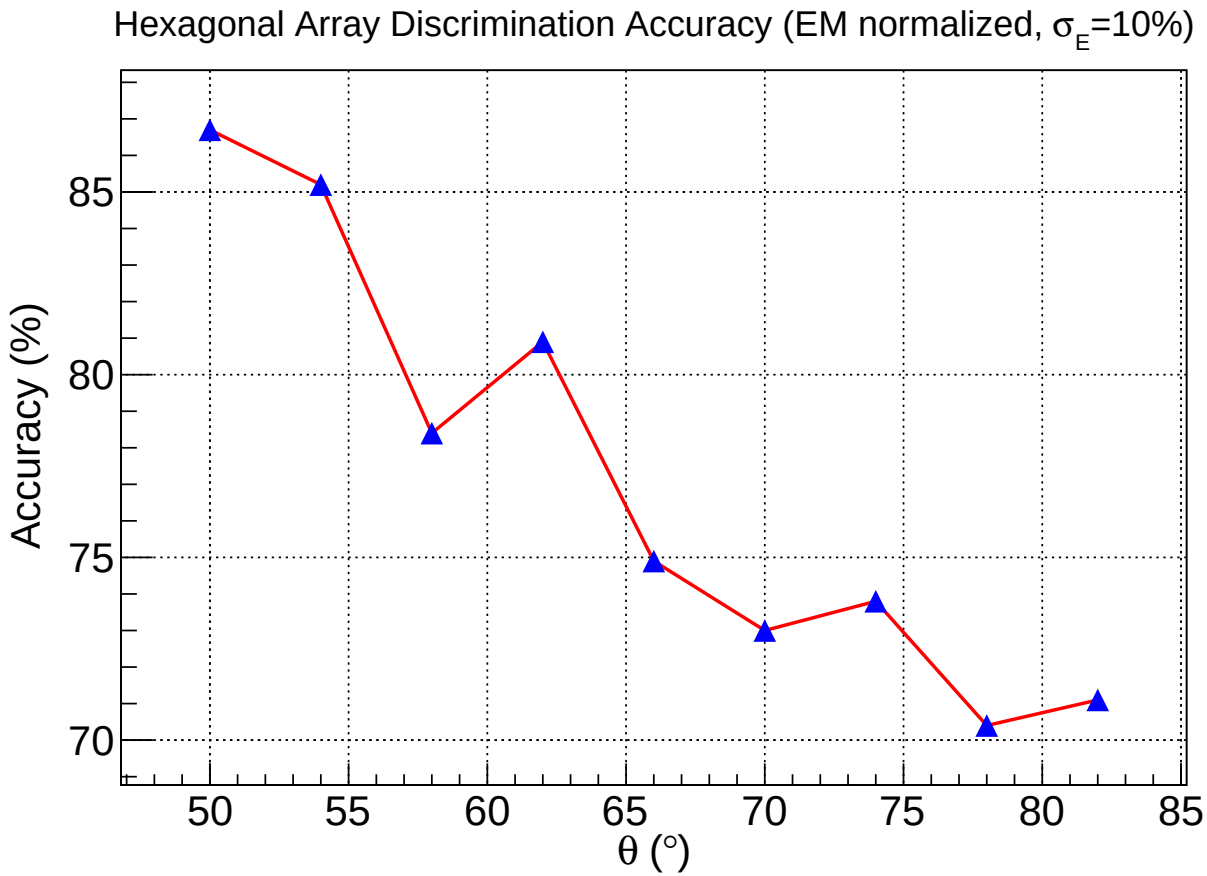

UNIVERSITY OF WARSAW

Why does the amplitude depend on X_{max} ?

- Vector potential contribution from a single finite particle track:

$$\vec{A}(t,\hat{u}) = \frac{\mu e}{4\pi R c^2}\vec{v}_\perp \frac{\Theta(t-t_1^{det})-\Theta(t-t_2^{det})}{1-n\vec{\beta}\cdot\hat{u}}, \qquad \vec{E} = -\frac{\partial \vec{A}}{\partial t} \quad \text{(ZHS formalism)}$$

- The Lorentz force constantly increases $\vec{v}_\perp$, but up to a limit due to the interactions of the charged particles with the air molecules
- This limit is governed by the drift velocity v_d, which is akin to a terminal velocity for $e^\pm$ in the air and is inversely proportional to ρ
- As X_{max} increases the shower develops lower in the atmosphere:
  - The density ρ increases with X_{max} , decreasing v_d and $\vec{v}_\perp$
  - The distance R to the array decreases with X_{max}
- This creates two competing effects! As X_{max} increases:
  - R decreases $\rightarrow |\vec{E}|$ increases
  - v_d decreases $\rightarrow \vec{v}_\perp$ decreases $\rightarrow |\vec{E}|$ decreases (geomagnetic emission)

Amplitude scaling with R

- The amplitude scales roughly with 1/R over the whole atmosphere
- By comparing simulations with and without the magnetic field on, we estimated the geomagnetic fraction of each shower
- By multiplying the Askaryan and Geomagnetic components by R, we can estimate the emission of each mechanism separately
- Since $E_{geo} \propto |\vec{B}| sin(\alpha)$, we also scale the geomagnetic component by $1/sin(\alpha)$ to account for changes in α as θ changes
- The magnetic field at GRAND is more than twice that at AUGER:
  - $|\vec{B}|_{Auger} = 24.0 \mu T$, $|\vec{B}|_{Grand} = 56.5 \mu T$
  - So, we expect to see a much higher geomagnetic emission at GRAND

UNIVERSITY OF WARSAW

Amplitude scaling with R

- Here we show the (scaled) average peak amplitudes at AUGER and GRAND as a function of zenith angle, for each emission mechanism
- The Askaryan emission is almost constant for all θ
- Much higher geomagnetic emission at GRAND than at AUGER
- But also, the geomagnetic emission increases much faster with zenith at AUGER than at GRAND. Why?

(Normalized by the Askaryan emission)

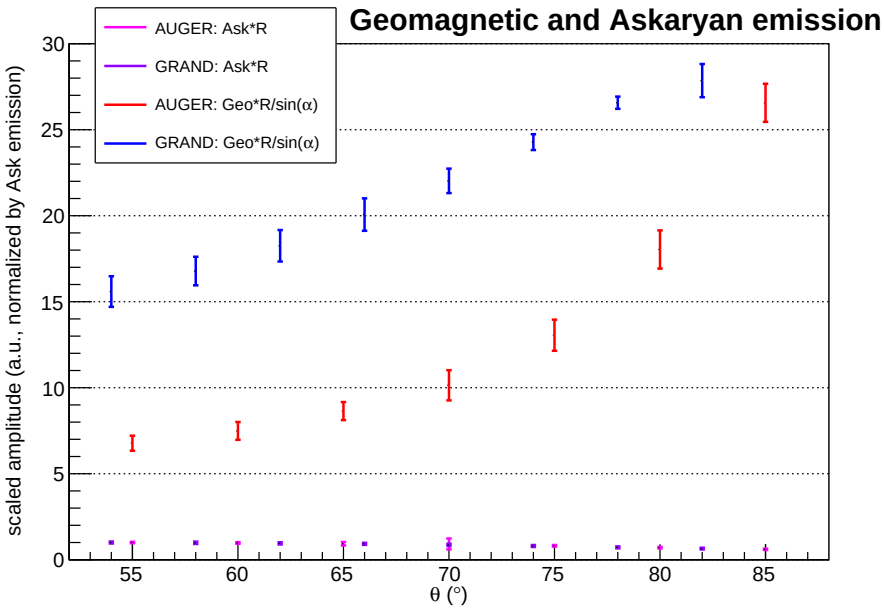

(Normalized by the Geomagnetic emission)

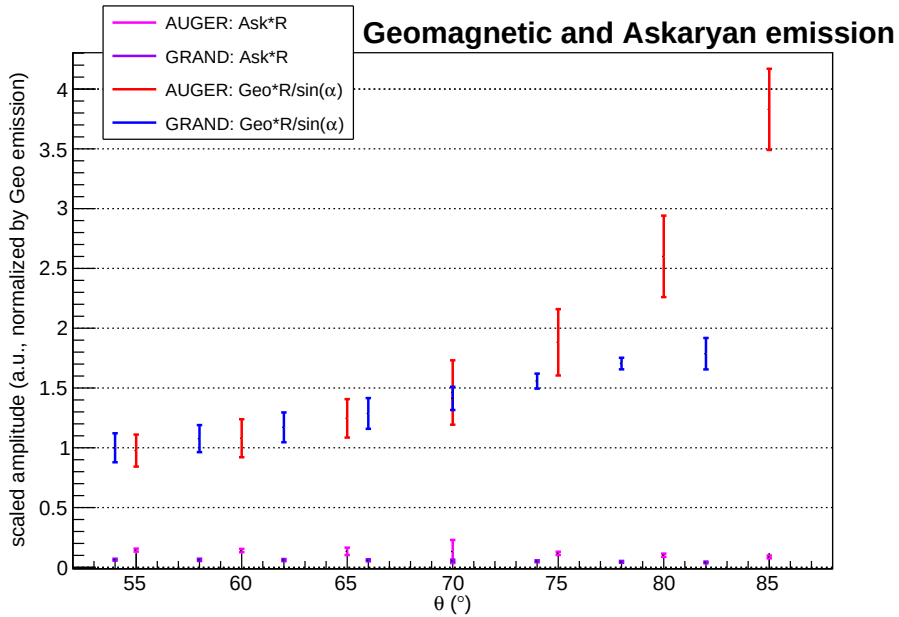

Loss of coherence at low air densities

- At lower densities (higher θ) the drift velocity v_d ($\propto 1/\rho$) increases
- So, the deflections due to the Lorentz force also increases
- Bigger deflections introduce extra time delays that lower the coherence of the radio emission (PRL 132, 231001, (2024) and JCAP08(2023)015)
- The loss of coherence increases with $|\vec{B}|$:
  - At GRAND, the higher geomagnetic field increases coherence loss
  - So, the geomagnetic emission increases less with θ at GRAND

(Normalized by the Askaryan emission)

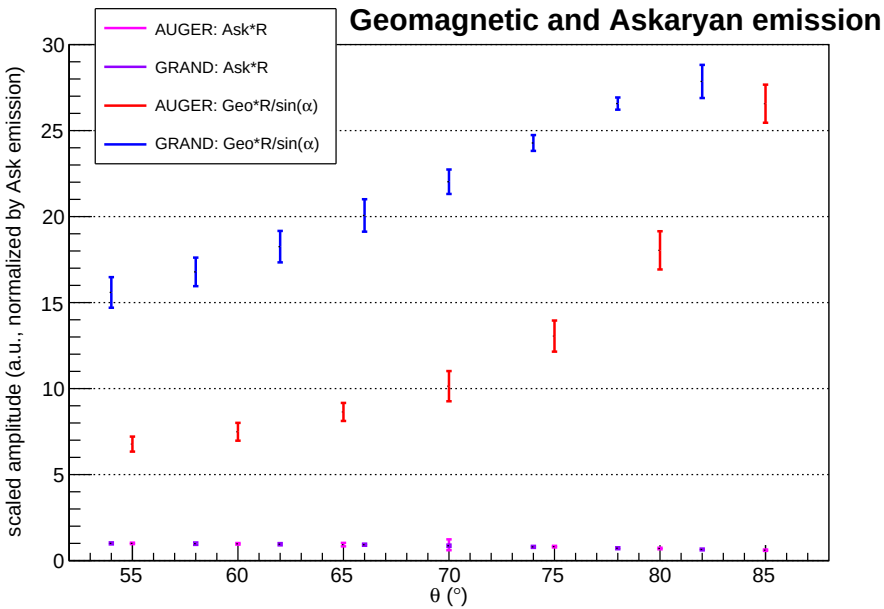

(Normalized by the Geomagnetic emission)

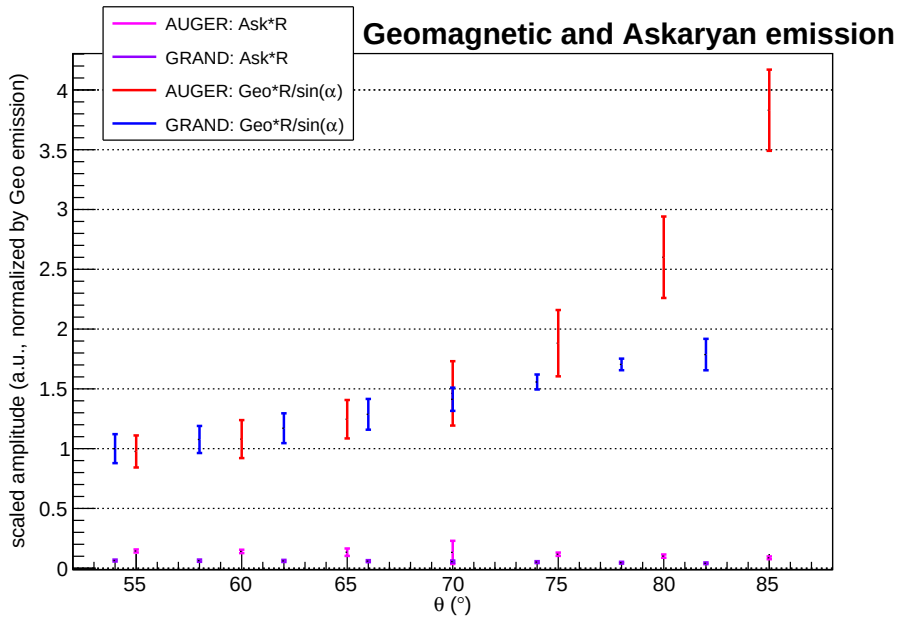

Amplitude scaling with the density ρ

- The geomagnetic emission scales very roughly with $1/\rho$
- This is due to the increase in v_d and $\vec{v}_\perp$ as the density ρ decreases
- But this scaling is linear only up to a certain point
- The $1/\rho$ becomes non-linear for higher θ (lower ρ), due to the increase in coherence loss
- The higher $|\vec{B}|$ is, the sooner the non-linearity appears
  - At GRAND, the linearity should break down at much lower zeniths θ
- At very low ρ and high $|\vec{B}|$, the $1/\rho$ scaling can actually reverse and $|\vec{E}|$ can instead start to decrease as ρ decreases
- Later we will quantify this loss of linearity with a factor $J(\theta)$
  - Change scaling: $(1/\rho) \rightarrow (1/\rho)^{J(\theta)}$

UNIVERSITY OF WARSAW

Amplitude scaling with the density ρ

- Here we show the inversely scaled geomagnetic component:
  - Geo$R(\rho/\rho_0)/\sin(\alpha)$
  - While the $(1/\rho)$ linearity holds, this value should be constant
- The $(1/\rho)$ scaling at AUGER is roughly linear up to $\sim 80°$, due to the smaller geomagnetic field leading to a smaller loss of coherence
- Due to the much higher $|\vec{B}|$ at GRAND, the $(1/\rho)$ scaling starts to loose linearity much sooner, at around 66°

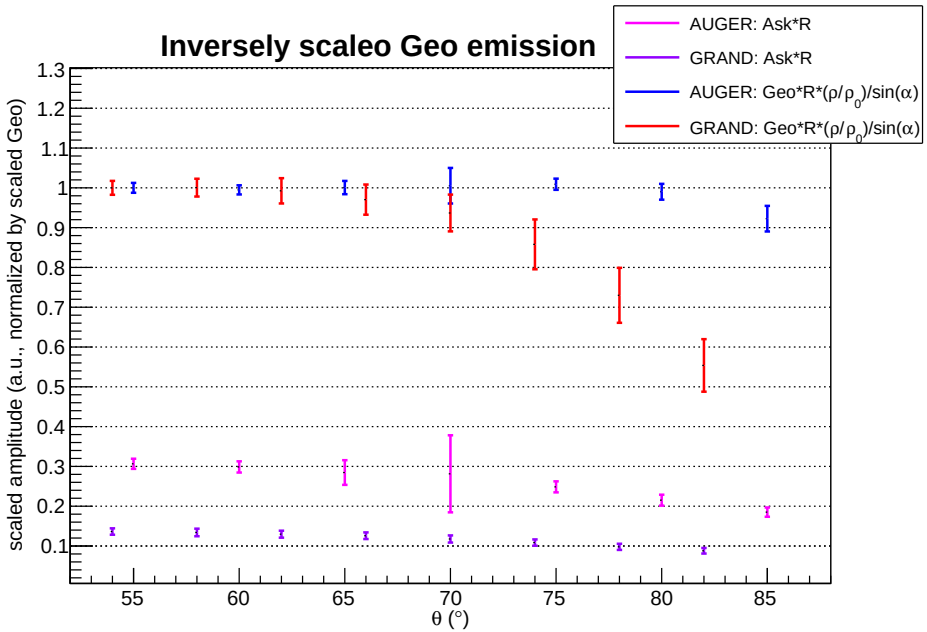

UNIVERSITY OF WARSAW

Estimating the ρ scaling non linearity

- Now we use a $(1/\rho)^{J(\theta)}$ scaling for the geomagnetic emission
- Fitted $J(\theta)$ from the simulation sets
- For $\theta > 76°$ at GRAND, the density scaling reverses!
- Decreasing the density now decreases the geomagnetic emission!

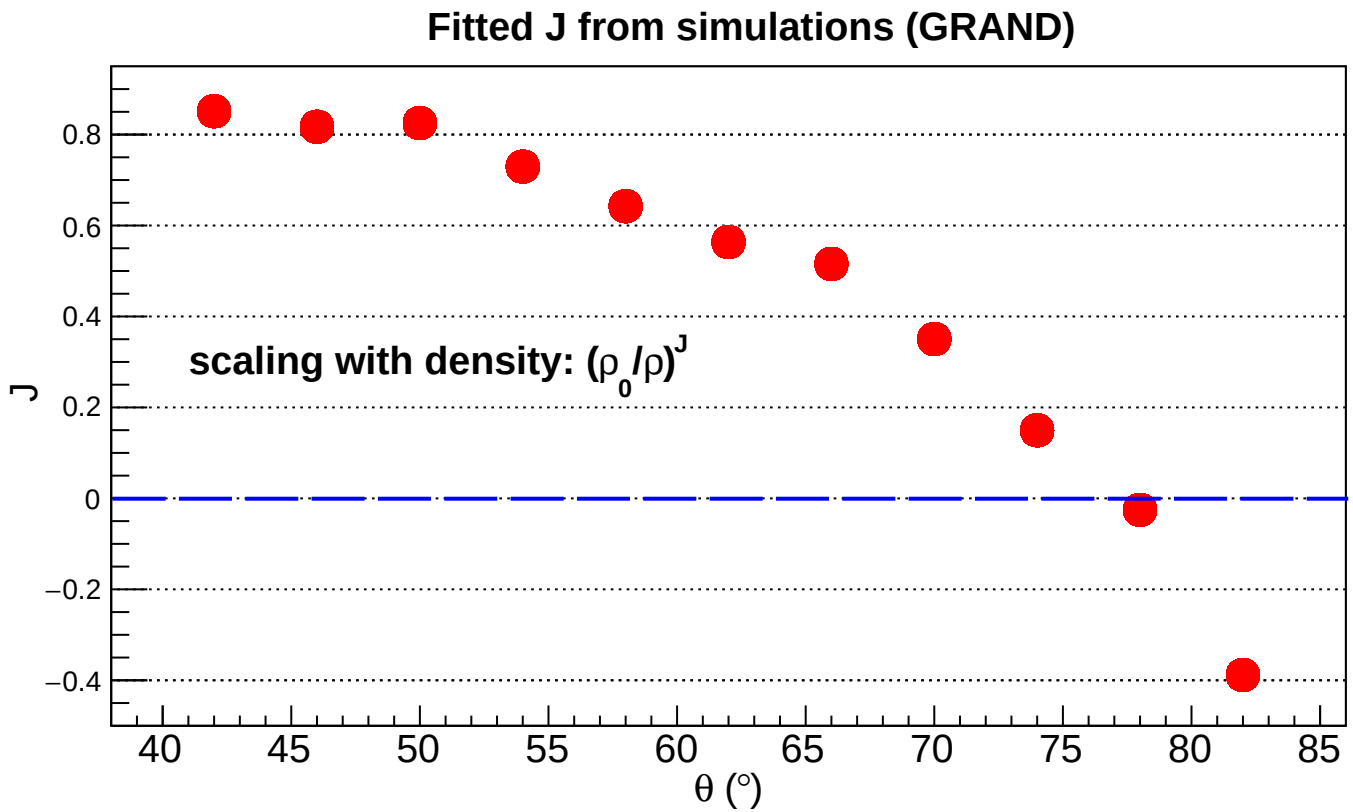

Which of the competing scalings wins?

- Protons tend to have higher X_{max} : lower R, but higher ρ than Fe
- The $1/\rho$ scaling tends to increase the field of Fe showers, while the $1/R$ scaling tends to increase the field of p showers
- Which effect dominates depends on the region in the atmosphere:
  - At low θ (high ρ) R varies more than ρ: R scaling wins
  - At higher zeniths (low ρ) ρ varies more than R: ρ scaling wins (if linear)
  - Nonlinear case: using $(1/\rho)^{J(\theta)}$ will diminish the effect of the ρ scaling

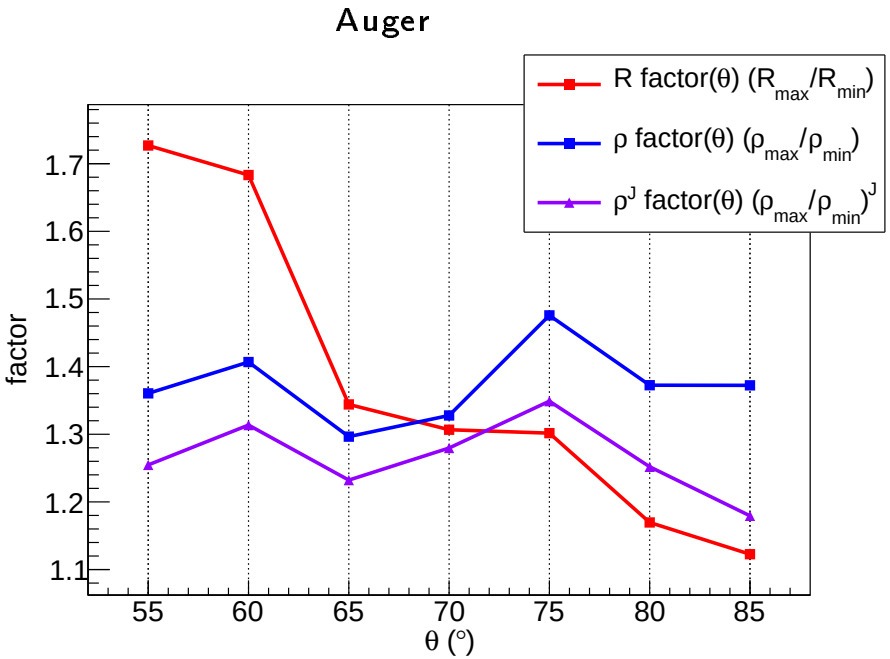

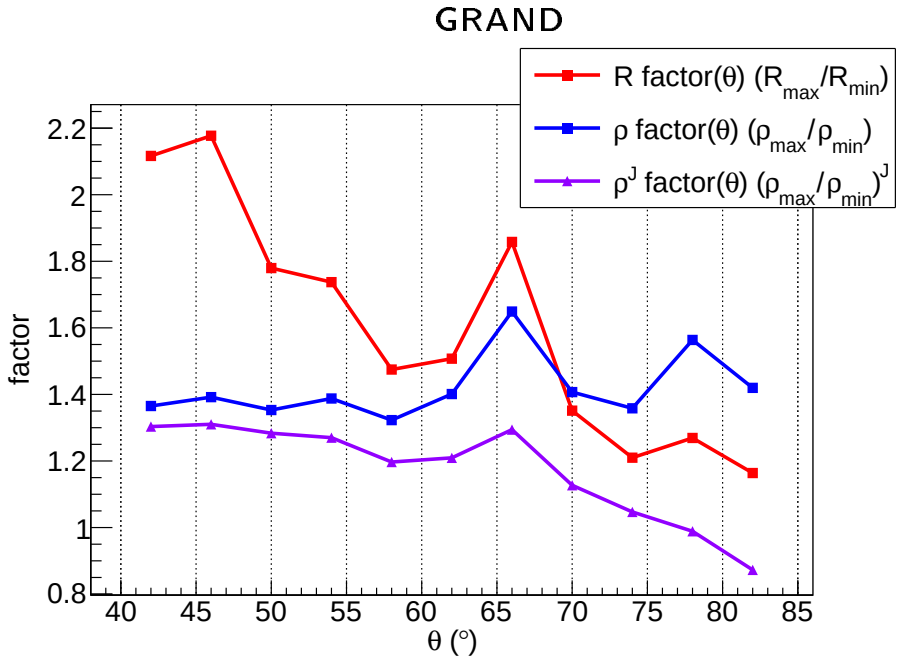

Site ($|\vec{B}|$) dependence: GRAND

- At GRAND, there is a greater loss of coherence due to the higher $|\vec{B}|$
  - This denies the increase of the $(1/\rho)^{J(\theta)}$ with zenith
  - The 1/R scaling dominates everywhere
  - Protons tend to have higher fields at every zenith, as observed

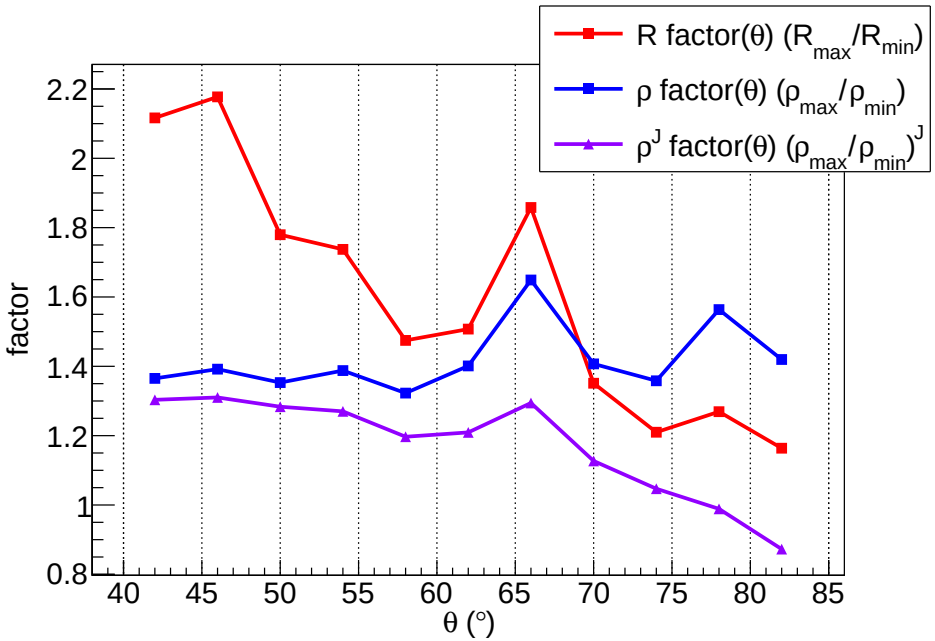

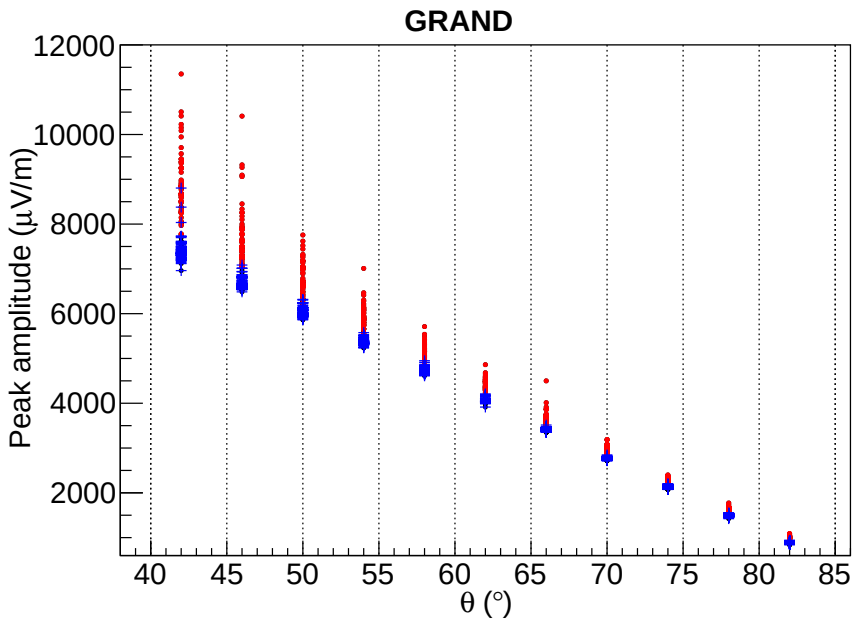

Site ($|\vec{B}|$) dependence: GRAND

- At GRAND, there is a greater loss of coherence due to the higher $|\vec{B}|$
  - This denies the increase of the $(1/\rho)^{J(\theta)}$ with zenith
  - The 1/R scaling dominates everywhere
  - Protons tend to have higher fields at every zenith, as observed

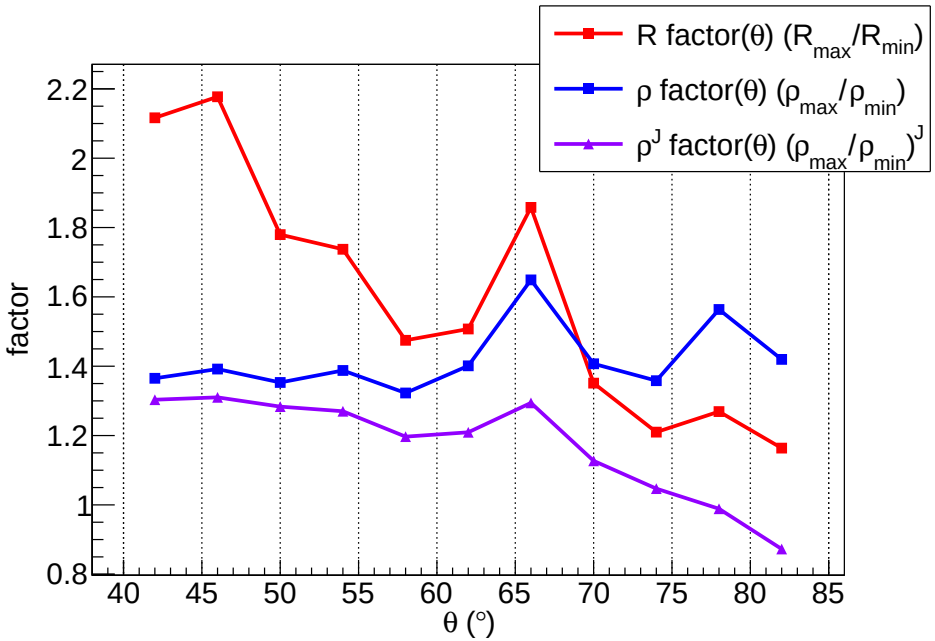

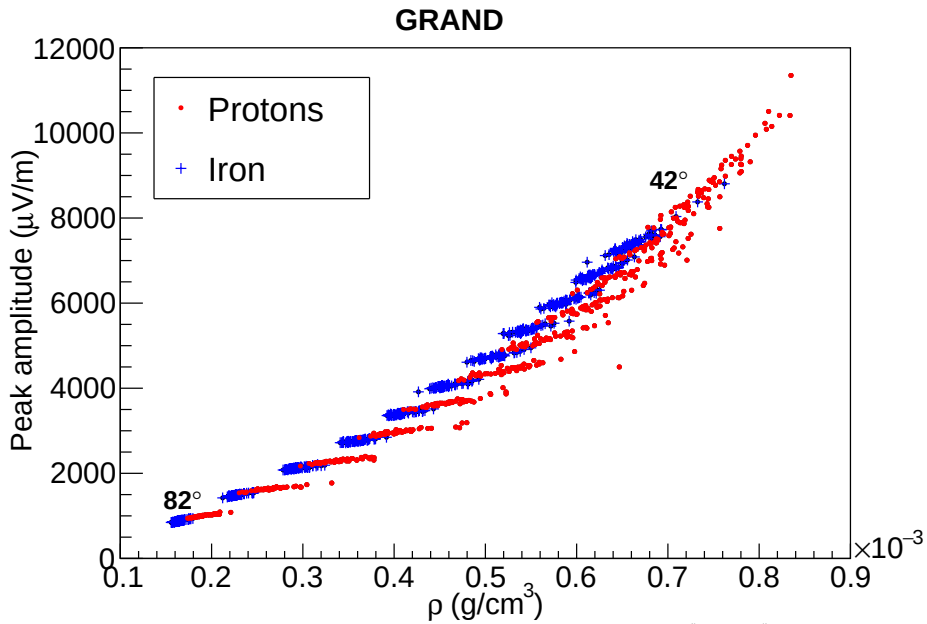

Site ($|\vec{B}|$) dependence: GRAND

- At GRAND, there is a greater loss of coherence due to the higher $|\vec{B}|$
  - This denies the increase of the $(1/\rho)^{J(\theta)}$ with zenith
  - The 1/R scaling dominates everywhere
  - Protons tend to have higher fields at every zenith, as observed

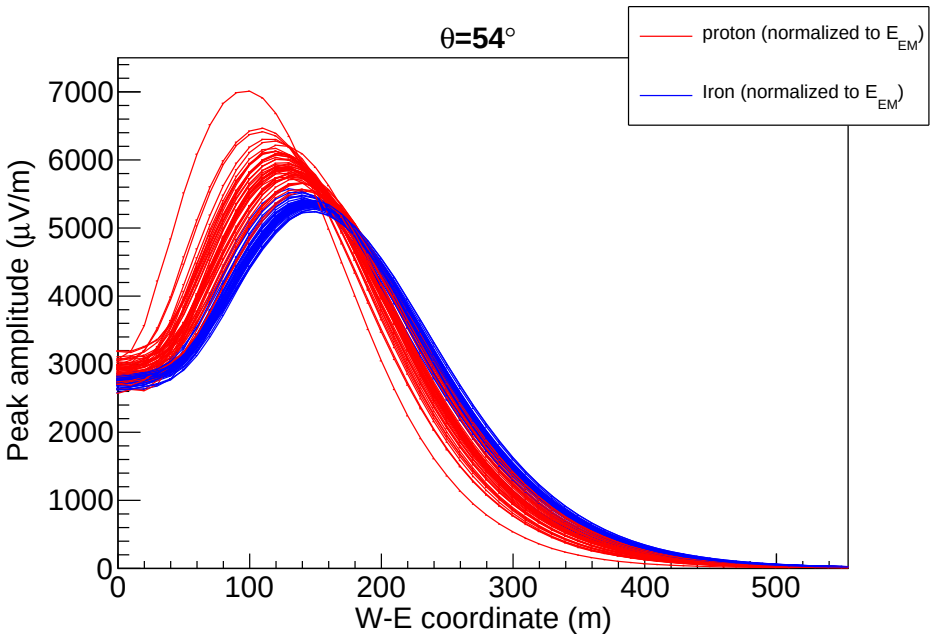

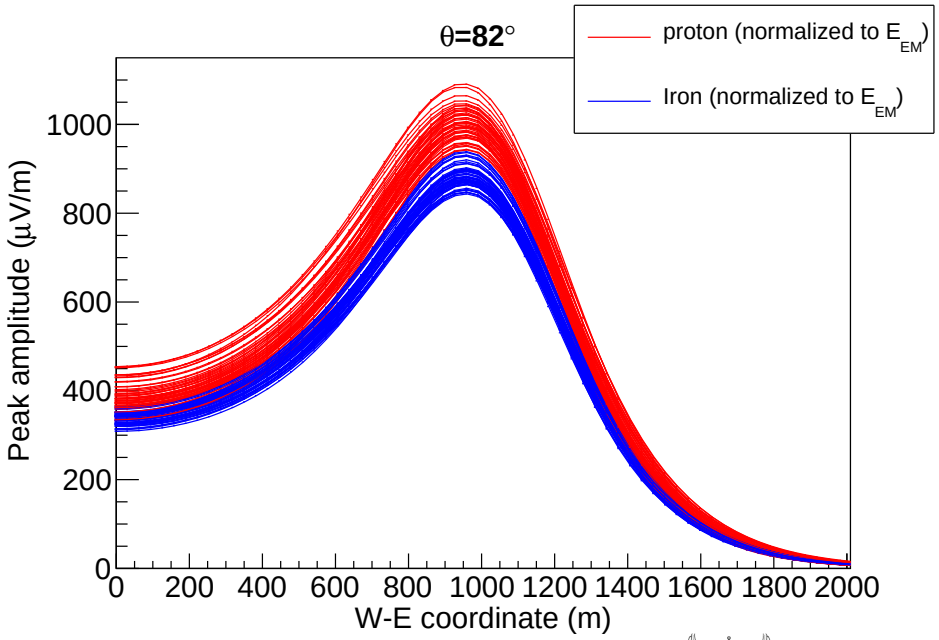

UNIVERSITY OF WARSAW

Site ($|\vec{B}|$) dependence: AUGER

- At Auger, there is a lot less loss of coherence (much lower $|\vec{B}|$)
  - The non-linearity term J diminishes less with zenith
  - So the $(1/\rho)^{J(\theta)}$ scaling starts to dominate for $\theta \gtrsim 72°$
    - Protons have higher fields for $\theta \lesssim 72°$
    - But Iron has higher fields for $\theta \gtrsim 72°$
    - The discrimination method should breakdown in this transition region

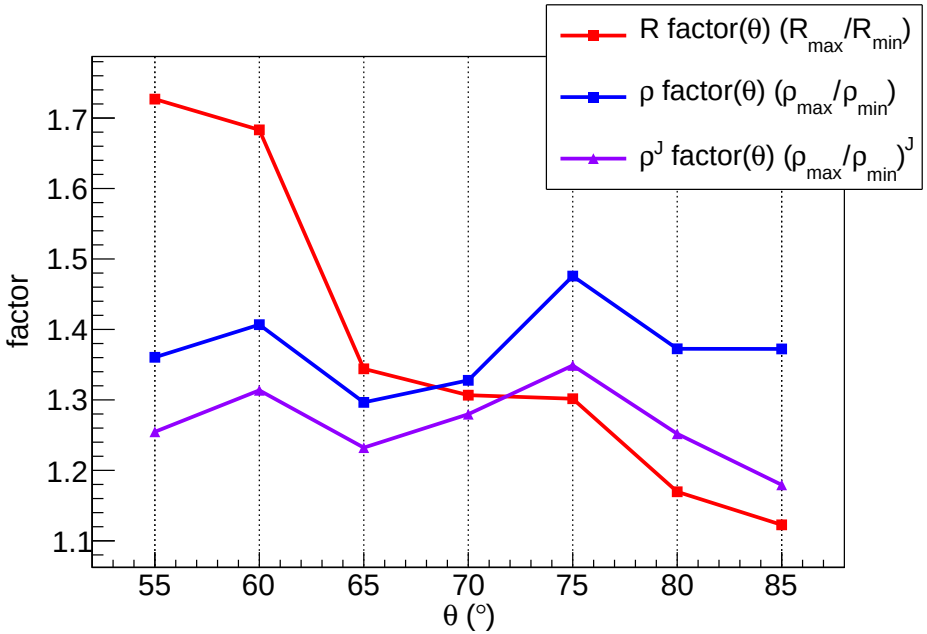

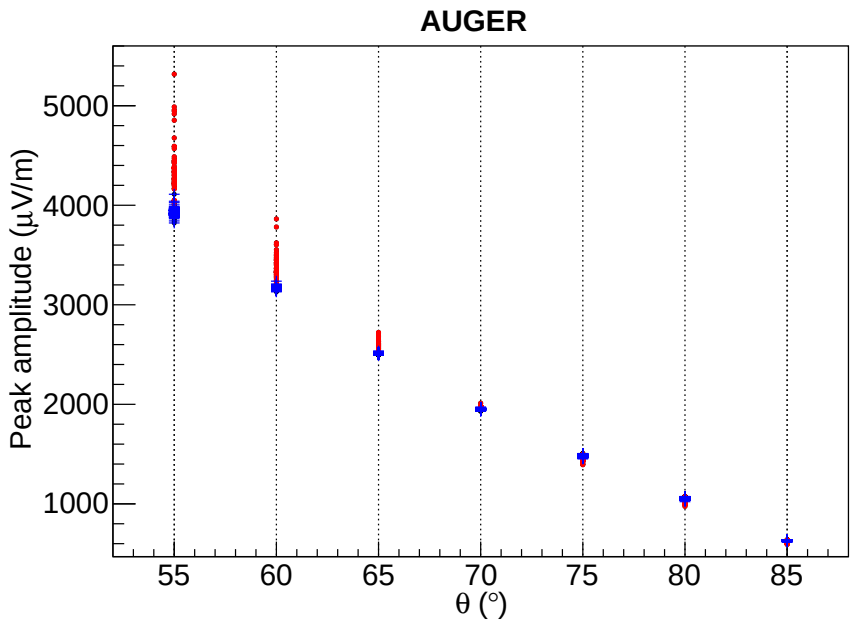

Site ($|\vec{B}|$) dependence: AUGER

- At Auger, there is a lot less loss of coherence (much lower $|\vec{B}|$)
  - The non-linearity term J diminishes less with zenith
  - So the $(1/\rho)^{J(\theta)}$ scaling starts to dominate for $\theta \gtrsim 72^\circ$
    - Protons have higher fields for $\theta \lesssim 72^\circ$
    - But Iron has higher fields for $\theta \gtrsim 72^\circ$
    - The discrimination method should breakdown in this transition region

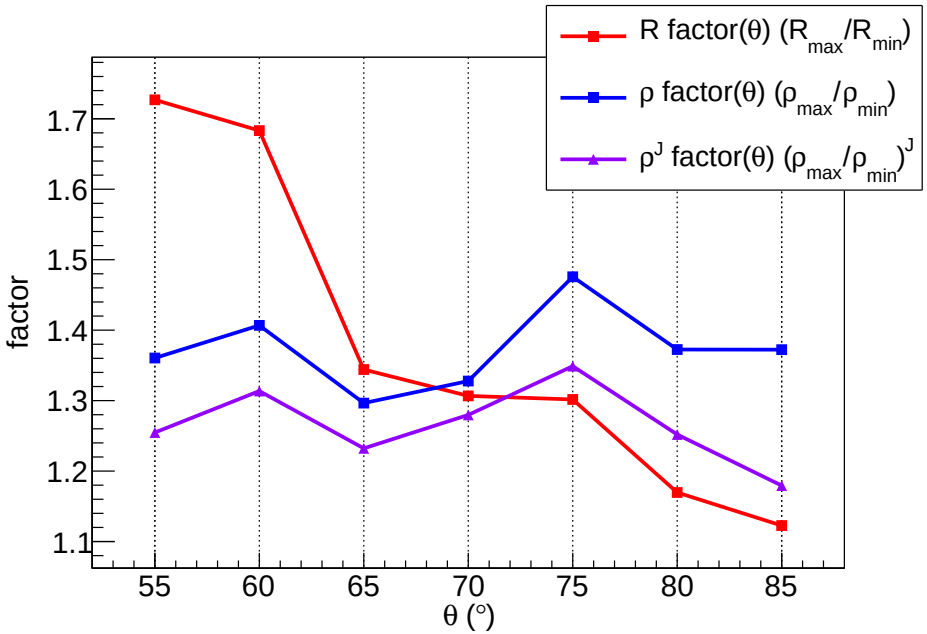

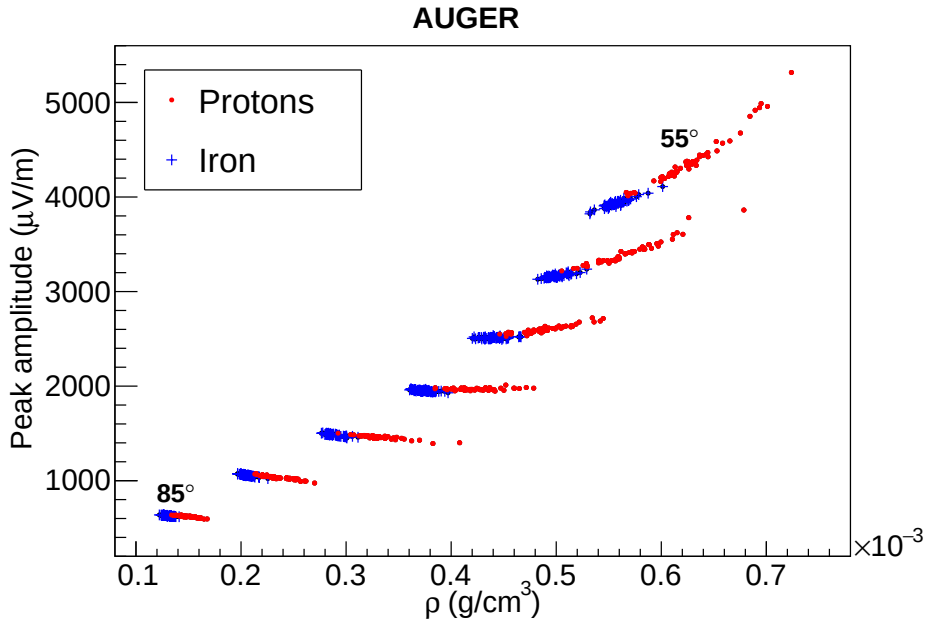

Site ($|\vec{B}|$) dependence: AUGER

- At Auger, there is a lot less loss of coherence (much lower $|\vec{B}|$)
  - The non-linearity term J diminishes less with zenith
  - So the $(1/\rho)^{J(\theta)}$ scaling starts to dominate for $\theta \gtrsim 72^\circ$
    - Protons have higher fields for $\theta \lesssim 72^\circ$
    - But Iron has higher fields for $\theta \gtrsim 72^\circ$
    - The discrimination method should breakdown in this transition region

Auger $\theta = 70^\circ$

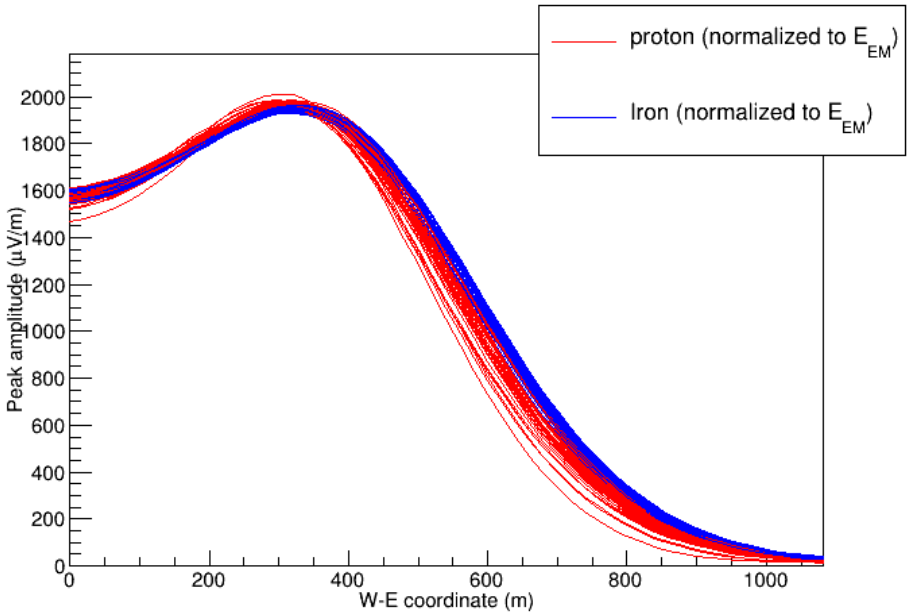

Auger $\theta = 75^\circ$

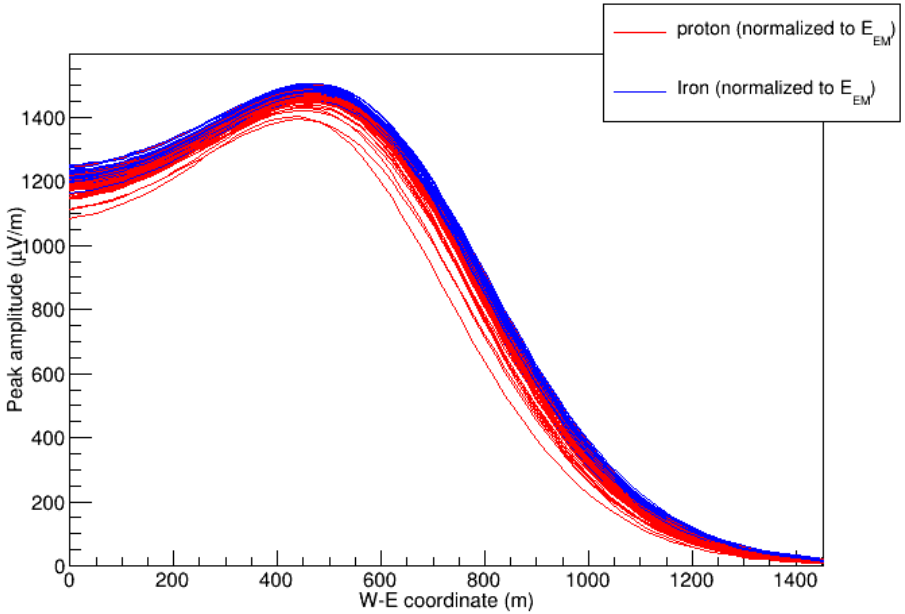

Conclusions

- There is a strong dependence of the radio LDF on composition
- It is much bigger than any EM energy differences between p and Fe
- We have also shown that this composition dependence can be understood in terms of two simple competing scalings:
  - A 1/R and a $(1/\rho)^{J(\theta)}$ scaling of the electric field, where $J(\theta)$ is a nonlinearity parameter fitted to the simulations
- The degree of loss of coherence at low densities (high zeniths) heavily depends on the geomagnetic field $\vec{B}$ at the detector site
- Higher magnetic fields will make the $(1/\rho)^{J}$ scaling loose linearity faster with increasing zenith ($J(\theta)$ decreases faster with θ)
- At GRAND, proton induced showers tend have higher measured electric fields for all zenith angles due to the huge $\vec{B}$ (lucky us!)
- The much lower $\vec{B}$ at AUGER creates a transition region at $\theta \simeq 72^{\circ}$
  - For $\theta \lesssim 72^{\circ}$, the 1/R scaling dominates and proton induced showers tend to have higher fields
  - For $\theta \gtrsim 72^{\circ}$, the $(1/\rho)^{J}$ scaling dominates and now iron induced showers tend have the higher fields

Conclusions

- This historically overlooked characteristic of EAS radio emission can be used not only for the ML approach presented here, but also to create other composition discrimination and energy reconstruction methods.
- Composition discrimination can be done on an event-by-event basis!
- Outlook:
  - This composition dependence of the LDF also suggests that there could be a huge composition bias in the current energy reconstruction methods that use radio amplitude data.
  - The estimated EM energy resolution of these methods may be heavily underestimated, as the quoted 5% is smaller than the amplitude differences between p and Fe.
  - This composition bias should be investigated to be sure it is properly taken into account by these modern EM energy reconstruction methods

Questions?

Other applications of Radio...

UNIVERSITY OF WARSAW

Section 3

BACKUP

Abstract

Revisiting the Radio Lateral Distribution Function dependence on primary composition

Washington R. Carvalho Jr.[a]

[a] *Faculty of Physics, University of Warsaw, Ludwika Pasteura 5, 02-093 Warsaw, Poland*

Abstract

In this work we show that there is a strong primary composition dependence on the radio lateral distribution function (LDF) at ground level, even accounting for differences in the electromagnetic (EM) energy of the showers. This composition dependence can be explained in terms of two competing scalings of the measured electric field that depend on the position of the shower maximum ($X_{\rm max}$) in the atmosphere: One with $(1/\rho)^J$, where ρ is the air density at $X_{\rm max}$ and J is a non-linearity factor, that tends to decreases the geomagnetic emission of deeper showers. The other scales with $(1/R)$, where R is the distance from $X_{\rm max}$ to the core at ground, and instead increases the measured electric of deeper showers. At low zenith angles, the $(1/R)$ scaling is stronger and leads to larger measured electric fields in the case of lighter primary compositions. The picture at higher zenith angles, i.e., lower densities, is more nuanced and is highly affected by the geomagnetic field. In this region, the deflections due to the Loretz force are much larger and increase the perpendicular momenta of $e^{\pm}$, which would tend to increase the radio emission. But it also increases the time delays between the particle tracks, decreasing the coherence of the emission. This loss of coherence can slow down, or even reverse the increase of the radio emission with decreasing air density and can be represented by a non-linearity factor J, which will govern if lighter compositions will have higher or lower fields than heavy primaries at these higher zenith angles. This LDF composition dependence can be used to directly infer, even bypassing any $X_{\rm max}$ reconstruction, the primary composition on an event-by-event basis. It also raises questions about a possible strong composition bias on modern radio based (EM) energy reconstruction methods.

Keywords: Ultra-high energy cosmic rays, Extensive air showers, Radio emission, Mass composition
PACS: 95.85.Bh, 29.40.-n, 96.50.sd, 95.55.Jz

Discrimination accuracy for GP300 array

- Fair accuracies even with a huge 30% smearing in shower energy
  - Interplay between the size of the footprint (zenith) and the different antenna distances of the infill and outlier antennas
  - At $\sim 70^{\circ}$ there is a change in the detection regime:
    - Infill only triggers$\rightarrow$Full array triggers
  - These geometrical effects disappear if a hexagonal array with a single antenna distance is used

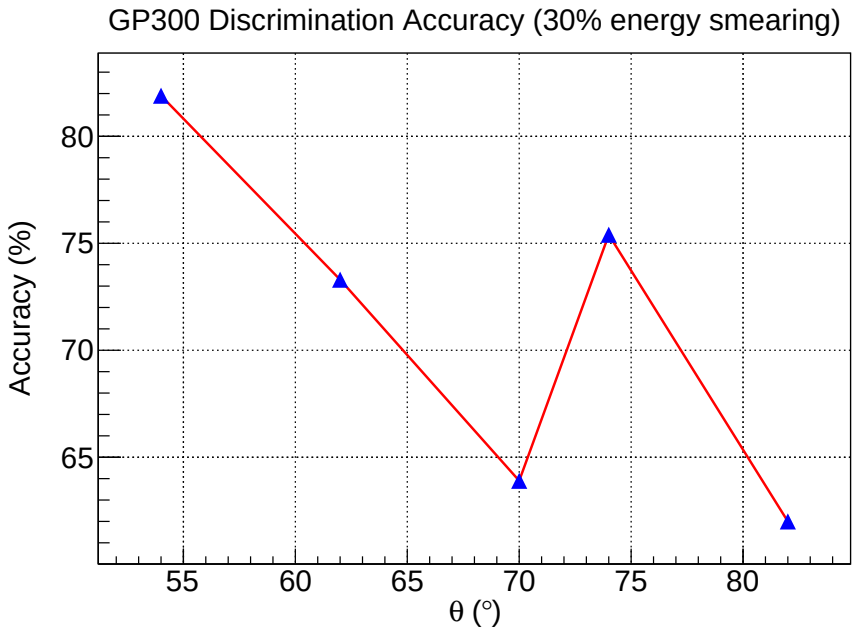

UNIVERSITY OF WARSAW

Superposition of emission mechanisms: Asymmetries

Vertical shower with horizontal $\vec{B}$

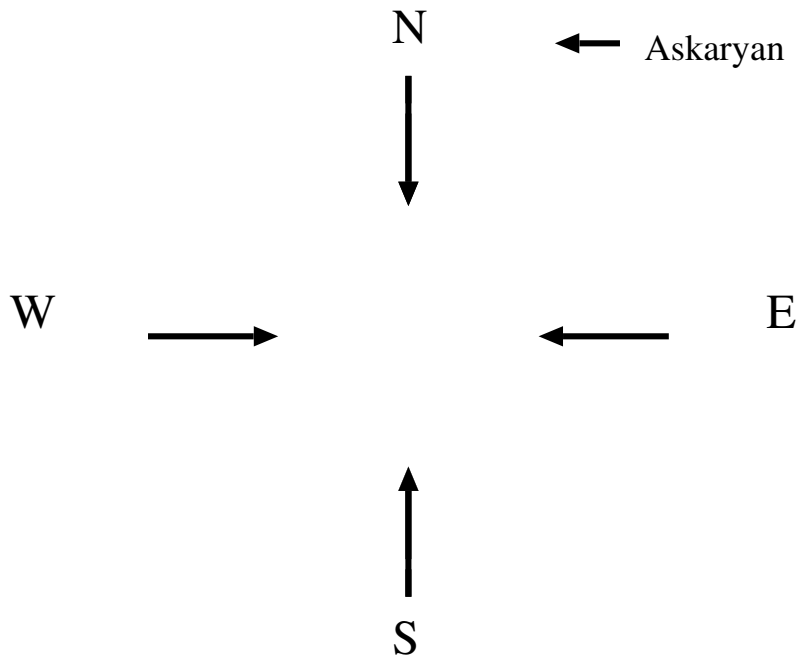

UNIVERSITY OF WARSAW

Superposition of emission mechanisms: Asymmetries

Vertical shower with horizontal $\vec{B}$

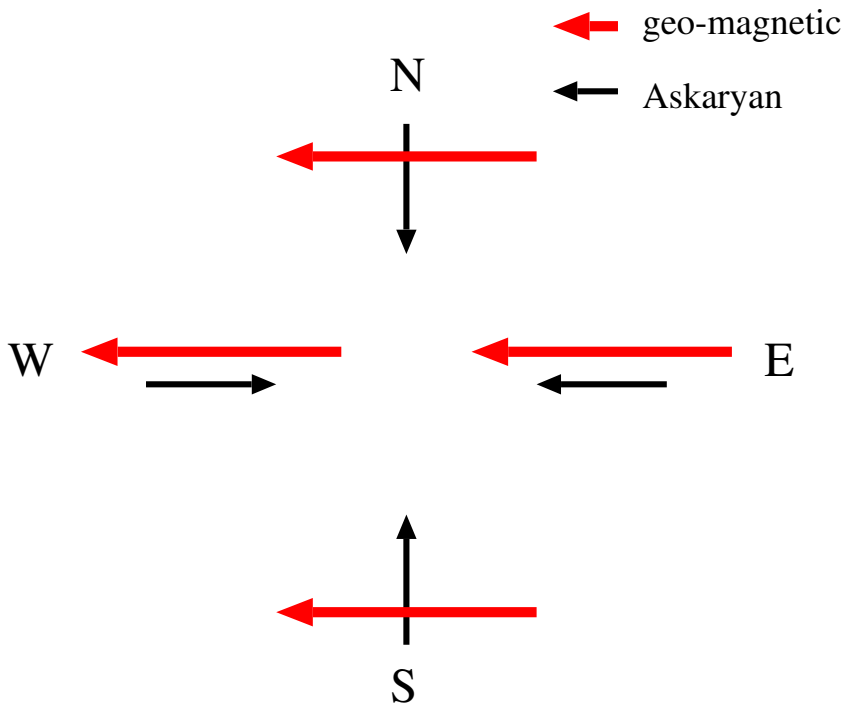

UNIVERSITY OF WARSAW

Superposition of emission mechanisms: Asymmetries

Vertical shower with horizontal $\vec{B}$

North of core

EW component: pure geomagnetic
NS component: pure Askaryan

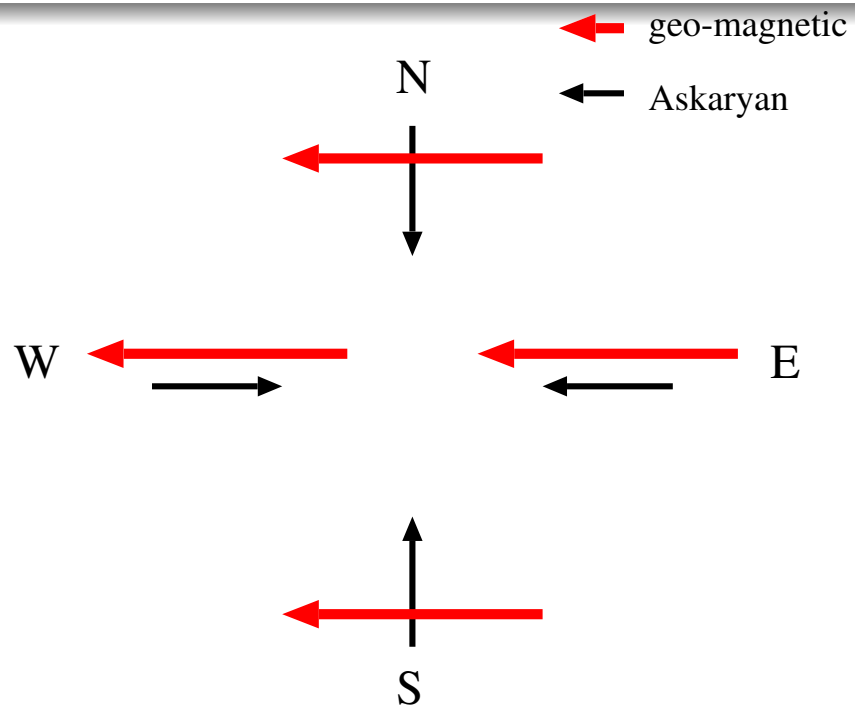

South of core

EW component: pure geomagnetic
NS component: pure Askaryan

UNIVERSITY OF WARSAW

Superposition of emission mechanisms: Asymmetries

Vertical shower with horizontal $\vec{B}$

North of core

EW component: pure geomagnetic
NS component: pure Askaryan

West of core

Askaryan and geomagnetic have **opposite** directions: They **subtract**

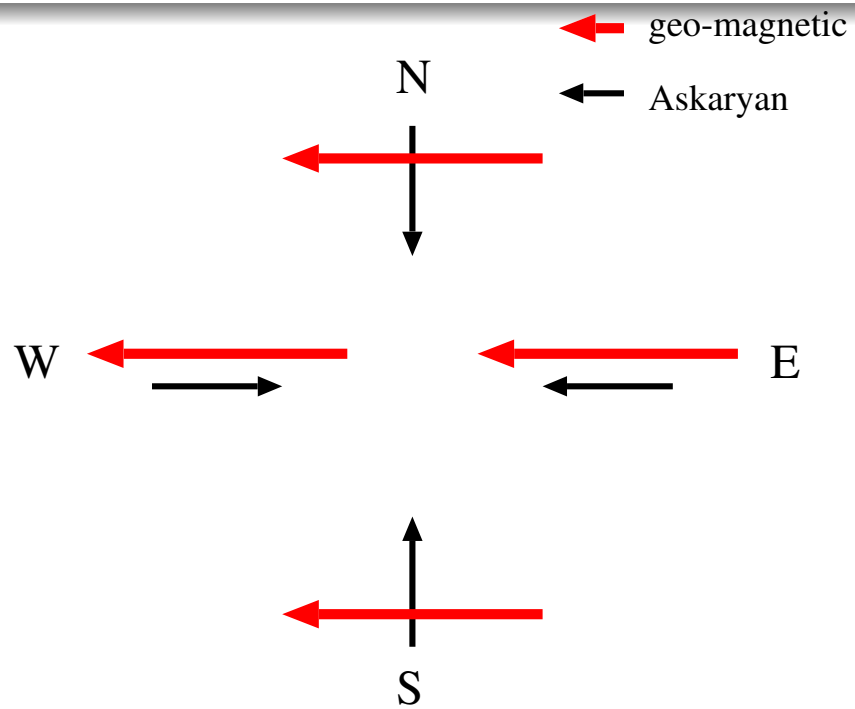

South of core

EW component: pure geomagnetic
NS component: pure Askaryan

UNIVERSITY OF WARSAW

Superposition of emission mechanisms: Asymmetries

Vertical shower with horizontal $\vec{B}$

North of core

EW component: pure geomagnetic
NS component: pure Askaryan

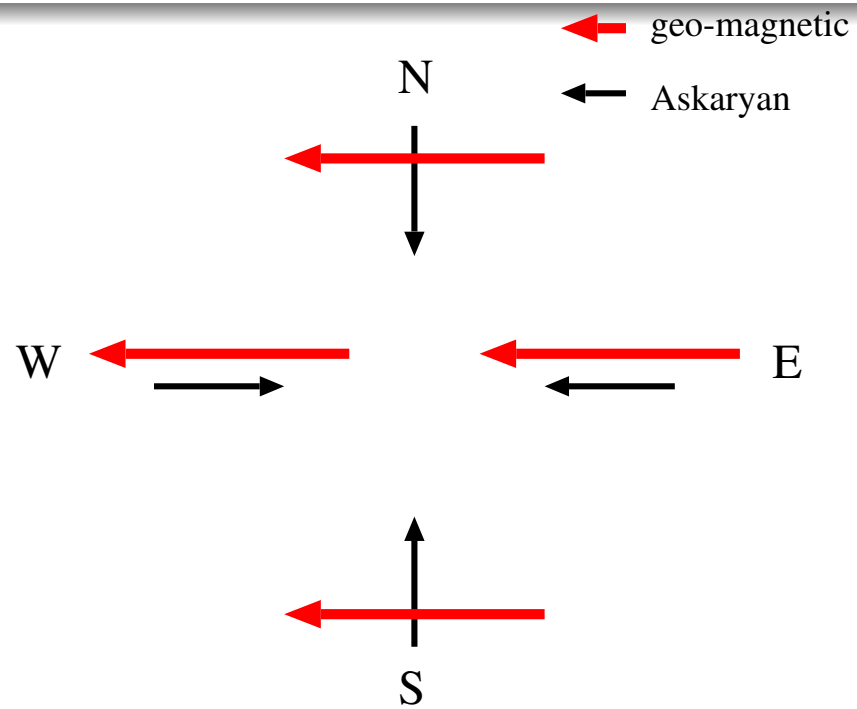

West of core

Askaryan and geomagnetic have **opposite** directions: They **subtract**

East of core

Askaryan and geomagnetic are parallel: They **add up**

South of core

EW component: pure geomagnetic
NS component: pure Askaryan

UNIVERSITY OF WARSAW

Superposition of emission mechanisms: Asymmetries

Vertical shower with horizontal $\vec{B}$

North of core

EW component: pure geomagnetic
NS component: pure Askaryan

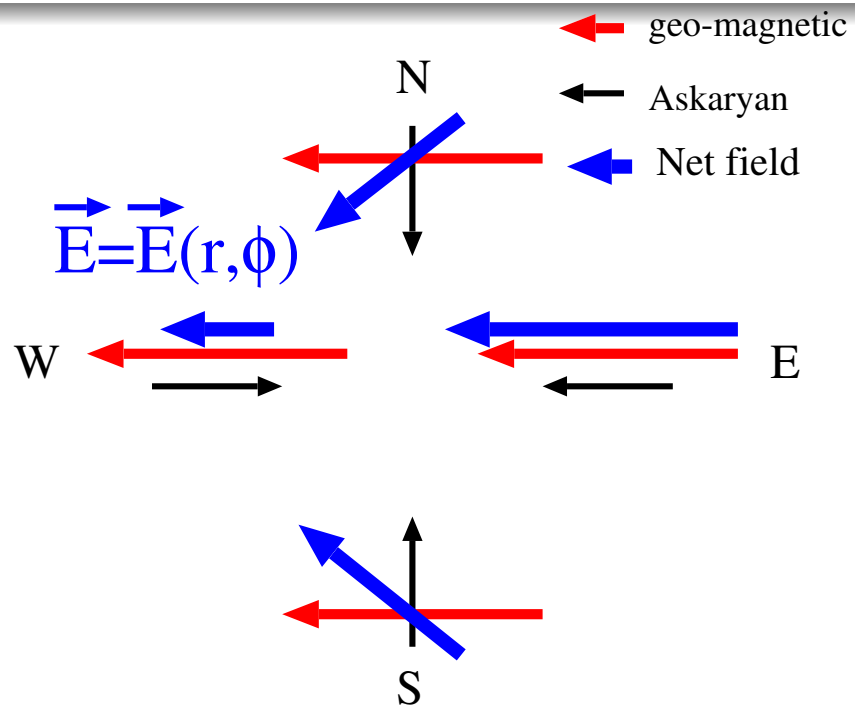

West of core

Askaryan and geomagnetic have **opposite** directions: They **subtract**

East of core

Askaryan and geomagnetic are parallel: They **add up**

South of core

EW component: pure geomagnetic
NS component: pure Askaryan

UNIVERSITY OF WARSAW

Superposition of emission mechanisms: Asymmetries

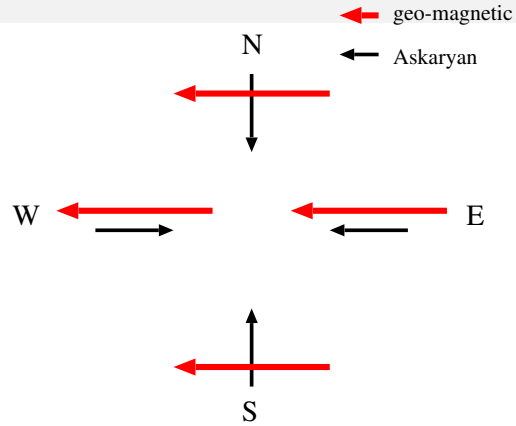

EW component

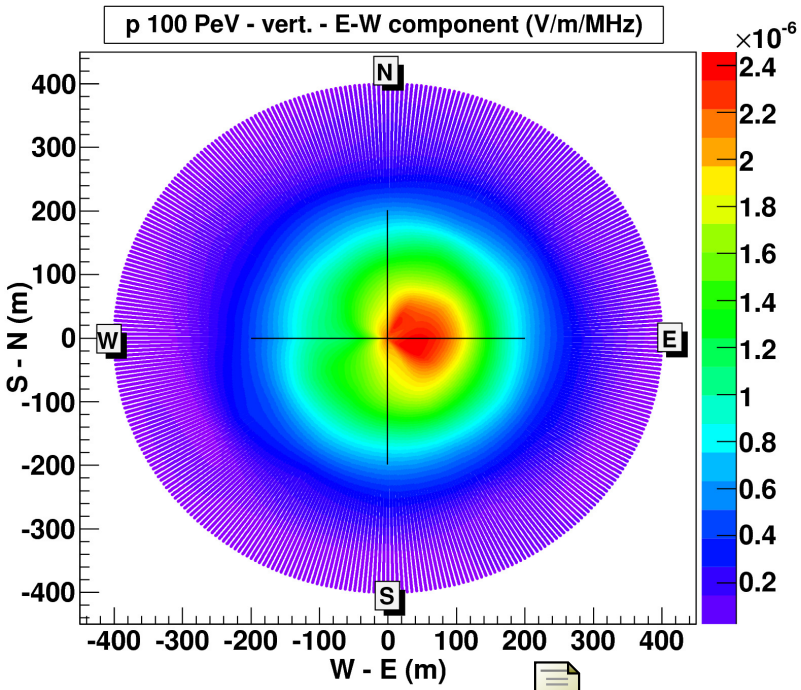

NS component

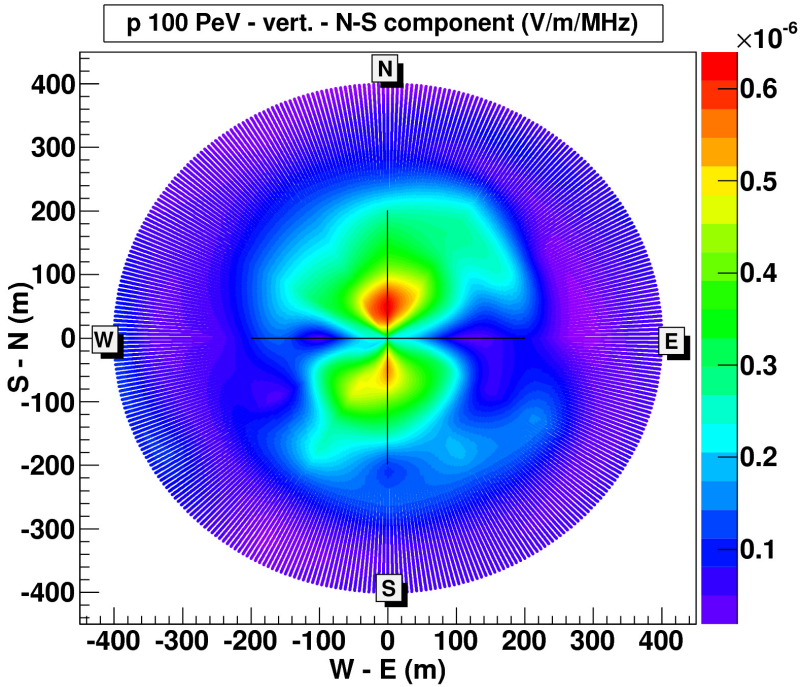

Atropar. Phys., **35**, (2012) 325

Dependence of the radio emission of air showers on the cosmic ray primary particle composition

We will start with brief introductions to Cosmic Rays (CR), extensive air showers and their radio emission. We will explore the origins of the dependence of the air shower development on the primary CR composition and how it affects the radio emission. We will then proceed to describe in more detail our newest work regarding a strong composition dependence on the measured radio signal amplitudes at ground level. This simple, yet historically overlooked dependence can be explained in terms of two competing scalings of the measured electric field that depend on the position of the shower maximum (X_{max}) in the atmosphere. This dependence can be used to directly infer the CR primary composition, even on a non-standard event-by-event basis.